

**UNCLASSIFIED**

**AD 444088**

**DEFENSE DOCUMENTATION CENTER**

**FOR**

**SCIENTIFIC AND TECHNICAL INFORMATION**

**CAMERON STATION, ALEXANDRIA, VIRGINIA**



**UNCLASSIFIED**

**NOTICE:** When government or other drawings, specifications or other data are used for any purpose other than in connection with a definitely related government procurement operation, the U. S. Government thereby incurs no responsibility, nor any obligation whatsoever; and the fact that the Government may have formulated, furnished, or in any way supplied the said drawings, specifications, or other data is not to be regarded by implication or otherwise as in any manner licensing the holder or any other person or corporation, or conveying any rights or permission to manufacture, use or sell any patented invention that may in any way be related thereto.

444088

CATALOGED BY DDC  
AS AD NO.

GDA-DBE-64-041  
Space Science Laboratory

FURTHER EXPERIMENTAL AND THEORETICAL STUDIES OF  
UNDEREXPANDED JETS NEAR THE MACH DISC

L. D'Attorre and F. Harshbarger

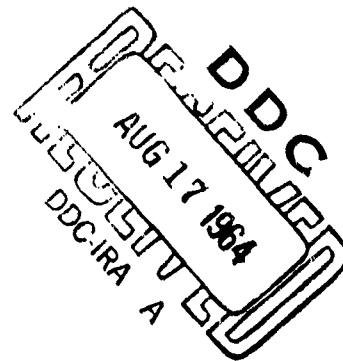
General Dynamics/Astronautics  
San Diego 12, California

Contract No. AF 19(628)-3269  
Program Code No. 3740  
ARPA Order 363 Amendment No. 3

July 1964

Prepared  
for

GEOPHYSICS DIRECTORATE  
AIR FORCE CAMBRIDGE RESEARCH LABORATORIES  
OFFICE OF AEROSPACE RESEARCH  
REDFORD, MASSACHUSETTS



**GD**

**GENERAL DYNAMICS | ASTRONAUTICS**

GDA-DBE-64-041  
Space Science Laboratory

FURTHER EXPERIMENTAL AND THEORETICAL STUDIES OF  
UNDEREXPANDED JETS NEAR THE MACH DISC

L. D'Attorre and F. Harshbarger

General Dynamics/Astronautics  
San Diego 12, California

Contract No. AF 19(628)-3269  
Program Code No. 3740  
ARPA Order 363 Amendment No. 3

July 1964

Prepared  
for

GEOPHYSICS DIRECTORATE  
AIR FORCE CAMBRIDGE RESEARCH LABORATORIES  
OFFICE OF AEROSPACE RESEARCH  
BEDFORD, MASSACHUSETTS

FURTHER EXPERIMENTAL AND  
THEORETICAL STUDIES OF UNDEREXPANDED  
JETS NEAR THE MACH DISC

L. D'Attorre and F. Harshbarger

ABSTRACT

Results of experimental flow visualization studies in the neighborhood of the Mach disc in underexpanded, inviscid jets are presented. The cases include sonic orifices, conical nozzles, Foelsch coordinate nozzles, and some full scale, in flight missile data. The exit to ambient static pressure ratios go up to 300 and the ambient Mach numbers go up to 4.3. In each case studied the method of Bowyer, D'Attorre, and Yoshihara appears to provide a reasonable technique for predicting the size and axial position of the Mach disc. In addition it is shown that the curvature in the Mach disc must be considered if a consistent triple point calculation is to be made.

CONTENTS

	<u>Page</u>
I. INTRODUCTION . . . . .	1
II. SUPERSONIC AMBIENT, HOT FLOW . . . . .	2
III. QUIESCENT AMBIENT, HOT FLOW, FOELSCH (A CORRECTION) . . . . .	4
IV. QUIESCENT AMBIENT, HOT FLOW, CONICAL . . . . .	5
V. QUIESCENT AMBIENT, COLD FLOW, SONIC ORIFICE . . . . .	9
VI. FLIGHT DATA . . . . .	12
VII. FLOW FIELD CALCULATIONS AND COMPARISONS . . . . .	14
VIII. CONCLUSIONS . . . . .	16
IX. REFERENCES . . . . .	17

FURTHER EXPERIMENTAL AND  
THEORETICAL STUDIES OF UNDEREXPANDED  
JETS NEAR THE MACH DISC

L. D'Attorre and F. Harshbarger

I. INTRODUCTION

Several different approaches for calculating the position and size of the Mach disc in underexpanded flows have been postulated. D'Attorre and Harshbarger<sup>1</sup> compared the results of a variety of different experimental conditions (including hot and cold flow as well as a quiescent and a supersonic ambient) with results calculated by the procedures of Bowyer, D'Attorre, and Yoshihara,<sup>2,3</sup> Adamson and Nicholls,<sup>4</sup> and Eastman and Radtke.<sup>5</sup> This initial comparison<sup>1</sup> indicated that the Bowyer, D'Attorre, and Yoshihara<sup>2,3</sup> approach provided results in better agreement with the varied experimental results than the other two approaches.<sup>4,5</sup>

Several additional experimental conditions have been treated recently which provide more justification for the initial conclusion and which resolve several problems which were brought to the attention of the authors. It is the purpose of the present report to document this additional work. Another report provides a complete summary of the results of this program.<sup>6</sup>

## II. SUPERSONIC AMBIENT, HOT FLOW

### A. Description of the Experimental Apparatus

A rocket engine with a Foelsch nozzle, an 8:1 expansion ratio, and burning gaseous oxygen and liquid RP-1 was studied. The nozzle exit diameter was 1.500 inches. The nominal total propellant flow rate was 0.695 lb/sec. The engine was operated at a nominal 500 psia chamber pressure and at a propellant mixture ratio of 2.25 to 1 ( $\text{GO}_2/\text{RP-1}$ ) by weight. The rocket was cooled by water and could be operated for more than an hour without damage. (The rocket nozzle was designated as Type II in the previous report.<sup>1</sup>)

The studies were carried out in the supersonic leg of the AEDC 16' x 16' propulsion wind tunnel. The rocket was fired axially, but about two feet above the center line. The products of combustion were removed by a scavenging system. The rocket jet was photographed through windows in the top of the wind tunnel by cameras operated remotely. The propellants were not doped with sodium.

### B. Experimental Conditions and Results

The engine was operated at a pressure altitude of 50,000 ft and at an ambient flow Mach number equal to 1.75. The photograph of this flow is presented in Figure 1. The calculated positions for the free stream shocks the jet boundary, and the jet shock structure have been superimposed on the photograph and on the same scale. The value of the axial distance divided by the nozzle exit diameter ( $X_m/d_e$ ) to the Mach disc as calculated by the technique of Bowyer, D'Atorre, and Yoshihara<sup>2,3</sup> is 6.3. The measured distance to the Mach disc is  $6.3 \pm 0.15$ . The calculated diameter of the Mach disc is 0.10 whereas the measured diameter of the Mach disc is  $0.1 \pm 0.003$ .

The flow field for nearly the same experimental conditions is provided in Figure 18. Also plotted in Figure 18 is the value of the pressure behind the incident shock as a function of the axial distance. According to the method of Eastman and Radtke<sup>5</sup> the position of the Mach disc occurs when this pressure is a minimum. The position so determined is  $X_{in}/d_e = 5.9$  which is 7% different from the experimentally determined value.

The same rocket engine was fired also at a pressure altitude of 66,500 ft with both a free stream Mach number of 2.15 and a quiescent ambient. These results, along with theoretical calculations for the same conditions, have been presented previously.<sup>1</sup> However, the quiescent ambient results were calculated incorrectly and have been corrected in Section III of this report.

### III. QUIESCENT AMBIENT, HOT FLOW, FOELSCH (A CORRECTION)

In Reference 1 consideration is given to an experiment in which the flow from an 8:1 area ratio nozzle (hot flow, Foelsch contour, nozzle Type II, see Section II) was photographed in an altitude tank at a pressure altitude of 66,500 ft. The photograph was reproduced as Figure 7 in Reference 1 with the correct dimensions indicated. However, in analyzing the result the nozzle exit diameter scale was misused. In Figure 2 of this report we provide the same photograph as was contained in Figure 7, Reference 1. Figure 2 contains lines for the position of the incident shock, Mach disc, reflected shock, and streamline at the triple point as calculated by the method of Bowyer, D'Attorre, and Yoshihara.<sup>2,3</sup> In Figure 14 of this report is given a calculated flow field along with a plot of the pressure ratio across the incident shock as a function of axial position and the position of the Mach disc as determined by the experiment, by the technique of Eastman and Radtke,<sup>5</sup> and by the technique of Bowyer, D'Attorre, and Yoshihara.<sup>2,3</sup> In Figure 3 are given the revised values for the various triple-point parameters (corresponding to Figure 20 in Reference 1).

It will be noted in Figure 14 that the axial position of the Mach disc determined theoretically is  $X_m/r_e = 21.4$ , by the technique of Bowyer, D'Attorre, and Yoshihara is 22.4, by the technique of Eastman and Radtke is 18.2, and by the technique of Adamson and Nicholls is 18.4.

#### IV. QUIESCENT AMBIENT, HOT FLOW, CONICAL

##### A. Description of Experimental Apparatus

A rocket engine with a conical 5:1 area ratio nozzle burning gaseous oxygen and sodium-doped gasoline was used to obtain photographs of an underexpanded jet in a quiescent ambient by Hendershot and Leo.<sup>7</sup> The exit and throat diameters were 0.366 inches and 0.164 inches, respectively. The nozzle half-angle was 15°. The total propellant flow rate was 0.045 lb/sec. The engine was operated at a nominal 340 psia chamber pressure and at a propellant mixture ratio of 1.8 (GOX to RP-1, by weight). The rocket was uncooled and was operated for approximately 2 seconds.

The studies were carried out in a 1000 ft<sup>3</sup> vacuum chamber, 6-ft in diameter and approximately 36-ft-long. The rocket was fired axially and photographed through a 12-in.-diam viewing port. The altitude tank was pumped down to 300 $\mu$  (approximately 185,000 ft pressure altitude) and the engine fired. The pressure altitude dropped from the initial value to 130,000 ft during the first second of the rocket run. Stable chamber pressure was achieved within 0.20 to 0.25 sec after ignition at which time the pressure altitude was approximately 150,000 ft.

A diaphragm-type differential pressure transducer was designed and fabricated. The pressure on both sides of the diaphragm was equilibrated before the run at the measured pressure altitude. Strain gauges were bonded to a cantilever beam which made contact with the diaphragm. The strain gauge output was calibrated for known, small, pressure differences. This pressure transducer was mounted inside the vacuum chamber, 3-ft directly below the rocket engine. The strain gauge outputs were recorded continuously during the run.

A 1% solution of sodium butyoxide mixed with the fuel provided satisfactory self-emission in the plume for photography at all altitudes.

A more complete description of this work has been given by Hendershot and Leo.<sup>7</sup>

B. Experimental Conditions and Results

Photographs were obtained at seven different pressure altitudes. The altitudes, photograph scale-factor, and so forth are given in Table I.

TABLE I. SUMMARY OF CONDITIONS

Figure No.	$p_a$ (mm Hg)	Pressure Altitude (feet)	$p_t/p_a$	Scale Factor for photos ( <u>photo scale</u> ) ( <u>model scale</u> ) (in./in.)
4	5.50	108,000	3200	0.258
5	3.90	117,000	4510	0.258
6	2.94	125,000	5960	0.258
7	1.84	135,000	9560	0.2295
8	1.70	137,000	10350	0.254
9	1.60	140,000	11000	0.254
10	1.05	150,000	16750	0.278

It will be noted in Figures 4 through 10 that the onset of the bright region indicating the position of the normal shock is curved, with the center of curvature away from nozzle exit. In all schlieren photographs which have been examined the curvature of the Mach disc is such that the center of curvature is located on the same side of the shock as the nozzle exit. This difference between a photograph of the self-emission and a schlieren picture was noted previously.<sup>1</sup> D'Attorre and Harshbarger<sup>1</sup> indicate that as the photographic exposure time is reduced by using a high

frame-rate movie camera the individual exposures show the shock to be flatter than is observed in photographs 4 through 10. Also the axial position of the shock changes from frame to frame in the experimental conditions they studied. It is believed that the effect of a somewhat unsteady shock position, when integrated over the 1/25 second exposure time in Figures 4 through 10 results in an apparent inverse curvature or shape for the Mach disc. The selection of the exact position for the stopping shock in Figures 4 through 10 was, as a result, somewhat arbitrary.

The values selected for the Mach disc position divided by the nozzle exit diameter ( $X_m/d_e$ ) are given in Table II. Also given in Table II

TABLE II. SUMMARY OF RESULTS

Figure No.	$p_e/p_a$	Mach Disc Axial Position $X_m/d_e$	Mach Disc Diameter $d_m/d_e$
4	97.0	19.0	7.9
5	136.5	24.0	10.1
6	181.0	27.0	13.2
7	290.0	31.0	15.6
8	313.5	32.0	15.7
9	333.8	37.7	16.9
10	506.0	39.5	19.5

are the values selected for the Mach disc diameter divided by the nozzle exit diameter ( $d_m/d_e$ ).

A calculation was made for the axial position of the Mach disc by two methods for the case given in Figure 9. In Figure 9 is superimposed the incident shock, the Mach disc, and the boundary as computed using the method of Yoshihara, D'Attorre, and Bowyer<sup>2,3</sup> and the pressure behind the incident shock as applicable to the method of Eastman and Radtke.<sup>5</sup> The technique of Adamson and Nicholls<sup>4</sup> should not be applied to this case

as it lies outside their bounds of validity.<sup>4</sup> A summary of the numerical results is given in Table III. Both theoretical approaches appear to

TABLE III. COMPARISON OF THEORIES WITH EXPERIMENT

	$\frac{x_m}{d_e}$	$\frac{d_m}{d_e}$
Experiment	37.7	16.9
Yoshihara, D'Attorre, and Bowyer <sup>2</sup>	40.0	18.7
Eastman and Radtke <sup>3</sup>	38.4	19.1

provide reasonable agreement for this particular experimental condition. Calculations were not made for the other experimental conditions.

## V. QUIESCENT AMBIENT, COLD FLOW, SONIC ORIFICE

Kawamura<sup>8</sup> conducted a number of experiments on underexpanded jets and attempted to explain the flow in the neighborhood of the triple-shock by using the usual triple-point relations. He reported good agreement for the cases in which the ambient to total pressure ratio ( $p_a/p_t$ ) is high. He reported one case in which  $p_a/p_t$  was relatively low for which the normal triple-point relations apparently fail. This case was brought to our attention by Adamson.<sup>2</sup> In order to determine the range of validity of the triple-point approach to the method of Bowyer, D'Attorre, and Yoshihara<sup>2,3</sup> this Kawamura case has been studied in some detail.

### A. Description of Experiment

Kawamura's experiments<sup>8</sup> were conducted with a 10-centimeter-diameter high pressure chamber which was terminated with a flat plate. An orifice was placed in the center of the flat plate. The orifice diameter was 22 millimeters and its circumference was beveled at  $45^\circ$  forming a sharp edge facing downstream. The working fluid was dry air. It was exhausted into the atmosphere. The jet structure was obtained by use of a schlieren apparatus. The Kawamura paper studied by the present authors did not contain schlieren photos suitable for analysis.

The present authors attempted to duplicate exactly the experimental apparatus of Kawamura. Results were obtained. However, the quality of the schlieren photographs obtained were not as good as those given by Ladenburg and Bershader<sup>9</sup> for a smaller sonic orifice diameter with nearly the same pressure ratio as the one which gave Kawamura trouble. The results obtained by the present authors and by Ladenburg and Bershader are similar. It is presumed that they agree also with the results obtained by Kawamura. The result presented by Ladenburg and Bershader<sup>9</sup> was obtained from apparatus described by Ladenburg, VanVoorhis, and Winckler.<sup>10</sup> The

working fluid is dry air. The sonic orifice diameter is 10 mm. Schlieren, shadowgraph, and interferometric visualization studies were made for pressure ratios throughout the range covered by Kawamura.<sup>8</sup>

#### B. Experimental Conditions and Results

Kawamura studied the triple-point relations for  $p_a/p_t$  equal to 0.320, 0.300, 0.190, and 0.175. It was at the lowest ratio of  $p_a/p_t$  (i.e., 0.175) that Kawamura found the triple-point relations invalid.

In Figure 11 is given the shadowgraph result of Ladenburg and Bershader<sup>9</sup> for a ratio  $p_a/p_t = 0.175$ . The photograph is excellent and shows clearly the curvature in the Mach disc. Also shown in Figure 11 are the lines resulting from a triple-point calculation made by the present authors.

The triple-point conditions were calculated using an estimate of the flow Mach number interpolated from the flow field properties given by Ladenburg, VanVoorhis, and Winckler.<sup>10</sup> The Mach number used is  $M_1 = 3.49$  which is slightly different from the one used by Kawamura ( $M_1 = 3.51$ ). We do not consider this an important difference because the triple-shock solution, in general, is not as sensitive to the value of the incident Mach number as it is to the shock angles. The local flow angle is determined from the experiment assuming the flow is source flow. The flow angle appears to be  $\theta_1 = 8^\circ$ . We assume the Mach disc is normal to the flow locally at the triple point. The tangent of the incident shock with respect to the flow at the triple shock is estimated to be  $\omega_1 = 35^\circ$ .

The triple point solution was obtained using graphs published in the Appendix of Reference 1 for  $\gamma = 1.4$  and  $M_1 = 3.49$ . The angle of the reflected shock with respect to the incident flow angle is calculated to be  $46.2^\circ$ . In summary, at the triple point the slip line angle is about  $8^\circ$ , the inclination of the incident shock with respect to the axis of the jet is  $27^\circ$ , the angle of

the reflected shock to the axis is  $46.2^\circ - (20.4 - 8^\circ) = 33.8^\circ$ . These angles have been traced on heavy lines in Figure 11 and show excellent agreement with the experiment, in contradiction of the comments of Kawamura.<sup>8</sup>

It is believed that Kawamura<sup>8</sup> failed to find valid triple-point conditions for this case because he assumed that the Mach disc was everywhere perpendicular to the axis of symmetry. As a result the relative angles between the incident, reflected, and Mach disc shock are not proper. The deviation from perpendicularity to the axis at the triple point (about  $8^\circ$  for this condition) is sufficient to introduce a discrepancy in the triple point calculations. At higher ratios of  $p_a/p_t$  the Mach disc is smaller, the curvature is less, and the slope of the Mach disc at the triple point is much more nearly normal to the axis. As a result, Kawamura was able to obtain valid triple-point relations for these less underexpanded conditions by assuming the shock was everywhere perpendicular to the axis.

## VI. FLIGHT DATA

### A. Description of Experiment

Excellent tracking photographic coverage is obtained on missiles during launch from the Western and Eastern Missile Ranges as standard operating procedure. For certain camera angles and missile altitudes the plume structure is quite well defined. The Thor and Jupiter missiles make use of the same single engine, 8:1 area ratio, semi-bell nozzle. The flow angle, static pressure, and Mach number are not uniform across the nozzle exit, but are roughly so. Therefore, it makes sense to study some of this field data. It provides a ready source of jet photographs with supersonic ambient flow. Unfortunately all the missiles fly roughly the same trajectory so that only a narrow range of experimental conditions (Mach number and pressure ratio) is obtained by this technique.

### B. Experimental Conditions and Results

A photograph for one set of conditions is presented in Figure 12. The aspect angle, ambient Mach number, and pressure ratio used for the data reduction are given on the figure.

It will be noted that it is impossible to determine the exact size of the Mach disc from this photograph. However, it is possible to estimate an upper limit for the diameter of the Mach disc. The axial position of the Mach disc can, in most cases, be located with fair accuracy.

The values for the axial position of the Mach disc and for the upper limit of its diameter are given for seven cases in Table IV. In Table IV  $p_e$  is the nozzle exit static pressure,  $p_a$  the ambient static pressure  $M_a$  the ambient Mach number relative to the missile,  $X_m$  is the axial distance to the Mach disc,  $d_m$  is the diameter of the Mach disc, and  $d_e$  is the diameter of the nozzle exit.

TABLE IV. SIZE AND POSITION OF MACH DISC TAKEN FROM FIELD DATA

Item	$p_e/p_a$	$M_a$	$X_m/d_e$	Upper limit for $d_m/d_e$
1	7.80	2.84	7.28±0.20	0.28
2	18.00	3.55	13.50±0.30	0.52
3	19.30	3.60	13.65±0.30	0.52
4	26.60	3.79	15.10±0.35	—
5	30.90	3.94	15.40±0.35	0.76
6	31.15	3.98	15.95±0.35	0.76
7	103.50	4.325	30.50±0.70	3.1

In Figure 23 is given the calculated flow field for nearly the same experimental conditions as Item 7, Table IV. Also in Figure 23 is given the variation of the static pressure behind the incident shock, and the position of the Mach disc as determined by the techniques of Bowyer, D'Attorre, and Yoshihara,<sup>2,3</sup> Eastman and Radtke,<sup>5</sup> and Adamson and Nicholls<sup>4</sup> (even though the latter technique should not be applied to the case of a supersonic ambient). The theoretical values obtained are 30.5, 21.0, and 30.0 (respectively) for  $X_m/d_m$ . The experimental value (see Table IV, Item 7) is approximately 30.5.

Surprisingly the technique of Adamson and Nicholls<sup>4</sup> provides a good estimate for the axial position of the Mach disc. The technique of Eastman and Radtke<sup>5</sup> provide a bad estimate. The method of Bowyer, D'Attorre and Yoshihara provides not only a good estimate for the axial position but also (within the accuracy with which the photo can be interpreted) for the diameter of the Mach disc.

## VII. FLOW FIELD CALCULATIONS AND COMPARISONS

The variety of experimental data available for study was limited. The results to date indicate that the technique of Bowyer, D'Attorre, and Yoshihara<sup>2,3</sup> provides a good estimate for the size and position of the Mach disc. As a result, a number of flow field calculations were undertaken for a variety of conditions for the purpose of comparing with the other two theoretical techniques.

Theoretical calculations were made for the inviscid flow field structure using the Bowyer program.<sup>11</sup> The three techniques for estimating the axial position (and size, where applicable) of the Mach disc were applied to these representative cases. The calculations were made assuming the flow is everywhere parallel to the axis at the nozzle exit, that the nozzle exit Mach number is equal to 3.185, and that the jet  $\gamma = 1.225$  and the ambient  $\gamma = 1.4$ .

In Figures 13 through 23 are provided the calculated lines of constant Mach number and the position of the various shocks and boundaries for several different arbitrary operating conditions. Also given is the variation of the pressure ratio across the incident shock, the position of the Mach disc and its size as calculated by the method of Bowyer, D'Attorre, and Yoshihara,<sup>2,3</sup> the axial position of the Mach disc as computed by the method of Eastman and Radtke,<sup>5</sup> and, where calculated, the axial position of the Mach disc as calculated by the method of Adamson and Nicholls.<sup>4</sup>

An analysis of Figures 13 through 23 indicates that the technique of Adamson and Nicholls<sup>4</sup> provides values for the axial position of the Mach disc which are in agreement with those predicted by the technique of

Bowyer, D'Attorre, and Yoshihara up to total to ambient static pressures ( $p_t/p_a$ ) equal to 650 for a quiescent ambient, but at greater pressure ratios the two techniques do not necessarily provide the same answer. The techniques of Eastman and Radtke<sup>5</sup> and Bowyer, D'Attorre, and Yoshihara<sup>2,3</sup> appear to give similar results for the axial position of the Mach disc for a static ambient but quite different results, in some cases, when there is a supersonic ambient.

### VIII. CONCLUSIONS

The importance of considering the curvature of the Mach disc in triple-point calculations has been indicated in analyzing the experimental results of Kawamura for fairly large exit to ambient pressure ratios ( $p_e/p_a$ ).

Additional experimental evidence has been obtained which indicates that the method of Eastman and Radtke cannot be relied upon to provide a correct answer for the size and axial position of Mach disc for all operating conditions.

No experimental conditions have been analyzed in which the technique of Bowyer, D'Attorre, and Yoshihara does not provide a reasonable estimate for the size and axial position of the Mach disc.

IX. REFERENCES

1. D'Attorre, L., and Harshbarger, F., "Experimental and Theoretical Studies of Underexpanded Jets Near the Mach Disc," General Dynamics/Astronautics Report GDA-DBE-008, 19 February 1964.
2. Bowyer, J., D'Attorre, L., and Yoshihara, H., "Transonic Aspects of Hypervelocity Rocket Plumes," Supersonic Flow, Chemical Processes and Radiative Transfer (Edited by Olfe and Zakkay) 201-210 Pergamon Press (1964).
3. Bowyer, J., D'Attorre, L., and Yoshihara, H., "The Flow Field Resulting from Mach Reflection of a Convergent Conical Shock at the Axis of a Supersonic, Axially Symmetric Jet," General Dynamics/Astronautics Report GDA 63-0586, 1963.
4. Adamson, T. C., Jr., and Nicholls, J.A., "On the Structure of Jets from Highly Underexpanded Nozzles into Still Air," Journal of Aero/Space Sciences, 16-24, (January 1959).
5. Eastman, D. W., and Radtke, L. P., "Location of the Normal Shock Wave in the Exhaust Plume of a Jet," AIAA Journal, 919, I (April 1963).
6. D'Attorre, L., and Harshbarger, F., "The Behavior of the Mach Disc Up to Moderate Pressure Ratios," General Dynamics/Astronautics Report GDA-DBE-042 (July 1964).
7. Hendershot, K. C., and Leo, P. P., "Scale Atlas Vernier Rocket Flame Expansion Studies," Convair, San Diego Report RT 59-105 (June 30, 1960).
8. Kawamura, R., "Shock Waves in Axially Symmetric Supersonic Jets," Tokyo University, Institute of Science and Technology, Report V. 6, No. 3 (June 1952) (translation available from NASA).

9. Ladenburg, R., and Bershader, D., "Interferometry," Chapter A, 3, Physical Measurements in Gas Dynamics and Combustion, Vol. IX of High Speed Aerodynamics and Jet Propulsion, Princeton University Press (1954).
10. Ladenburg, R., VanVoorhis, C. C., Winckler, J., "Interferometric Studies of Faster than Sound Phenomena. Part II. Analysis of Supersonic Jets," Physical Review, Vol. 76, No. 2, 662-677 (September 1949).
11. Bowyer, J., "Determination of the Envelopes and the Lines of Constant Mach Number for an Axially Symmetric Jet," General Dynamics/Astronautics Report ZJ-7-054 (March 1958).

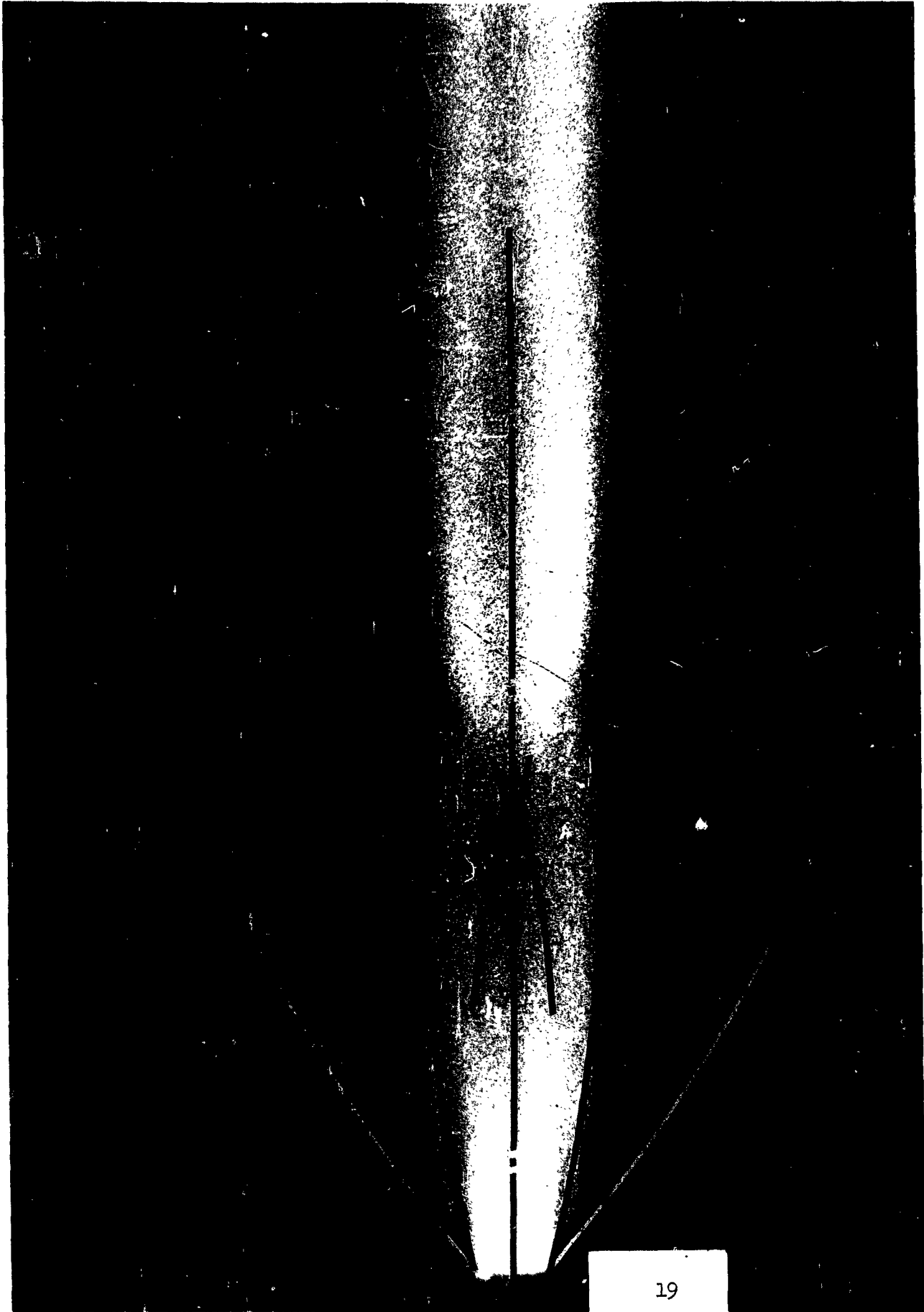


FIGURE 1. Photograph of a Rocket Operated with  $p_e/p_a = 4.68$  and a Freestream Mach Number = 1.75. Superimposed are lines corresponding to the calculated values for the ambient shock (white lines), jet boundary, jet shock, and Mach disc (black lines).

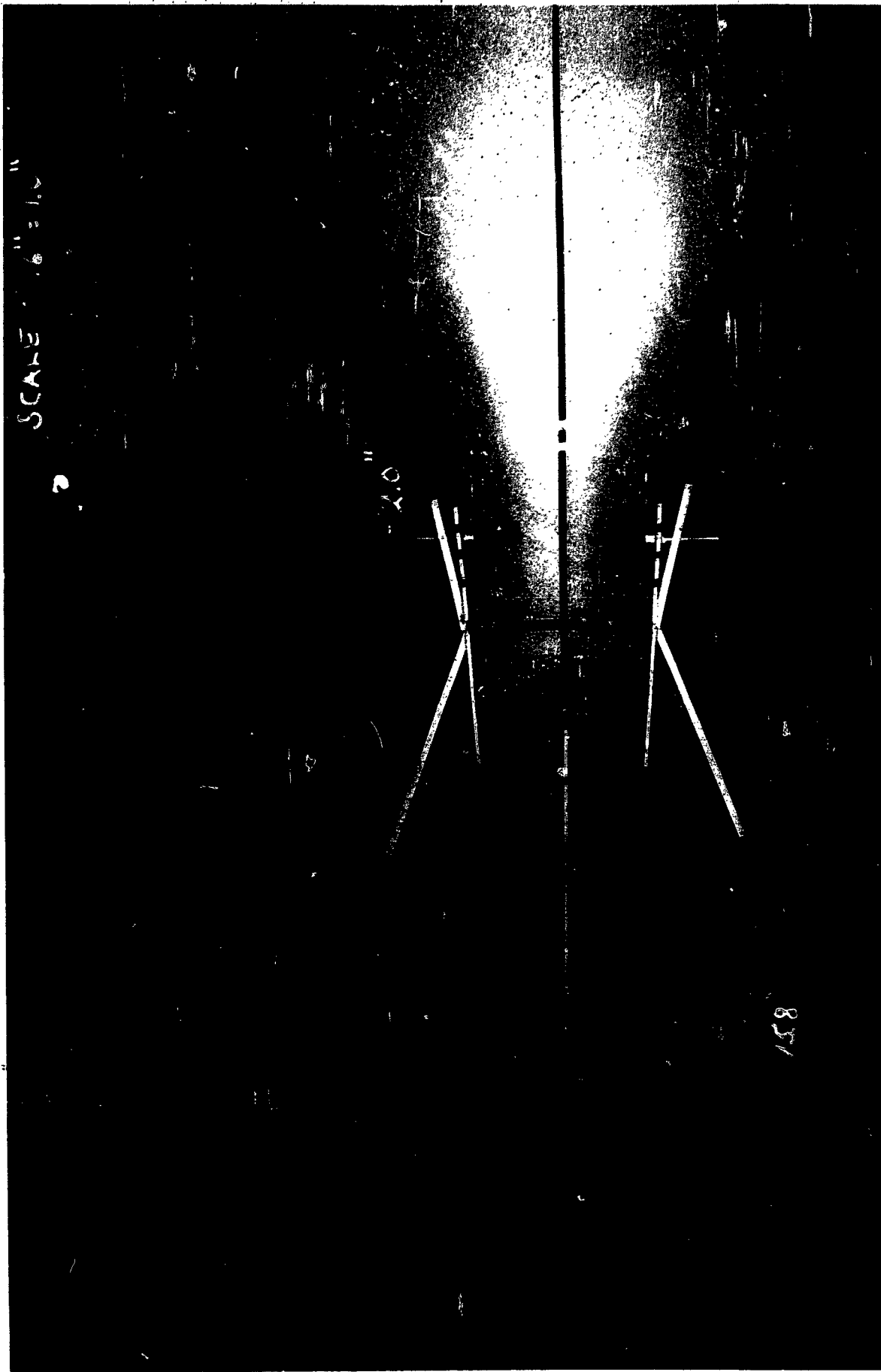
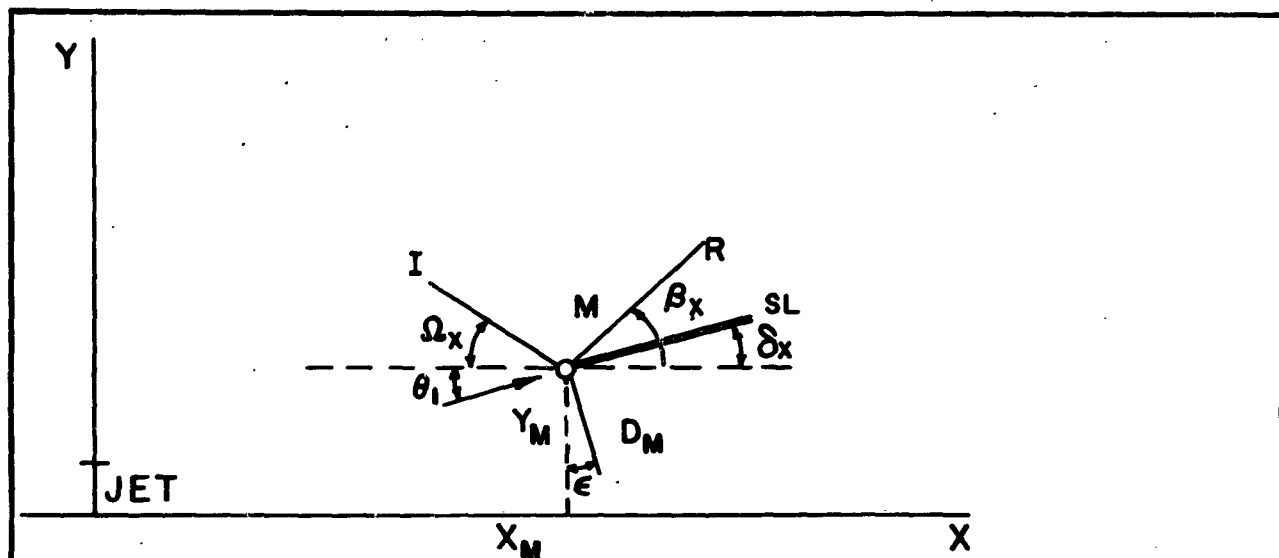


FIGURE 2. Photograph of a Plume with Rocket Operated with  $P_e/P_a = 10.3$  and a Static Ambient. Superimposed are the calculated positions for the incident and reflected shock (heavy white lines), the incident flow angle and slip lines (thin white solid and dashed lines) at the triple point, and the Mach disc (heavy black line). The flow is from left to right.



I - INCIDENT SHOCK.

R - REFLECTED SHOCK.

$D_M$  - MACH DISC SHOCK.

$X_M, Y_M$  - TRIPLE POINT COORDINATES.

THE DISTANCES ARE IN UNITS OF THE EXIT RADIUS  $r_j$ .

$M_s$	$X_M$	$Y_M$	$\theta_i$	$\Omega_x$	$\beta_x$	$\delta_x$	$\epsilon$	$d_M = 2Y_M$
0	23.4	1.4	4.0°	21.2°	12.6°	4.0°	4.0°	2.8

FIGURE 3. Triple-point Results (Revised) for a Rocket Operated with  $p_e/p_a = 10.3$  and a Static Ambient (see the photograph in Figure 2). This case was presented incorrectly in Reference 1.

$h = 66,500$  ft. , 8 : 1 AREA RATIO,  
 CHAMBER PRESS. 500 psi,  $\gamma_j = 1.225$ ,  $M_j = 3.17$

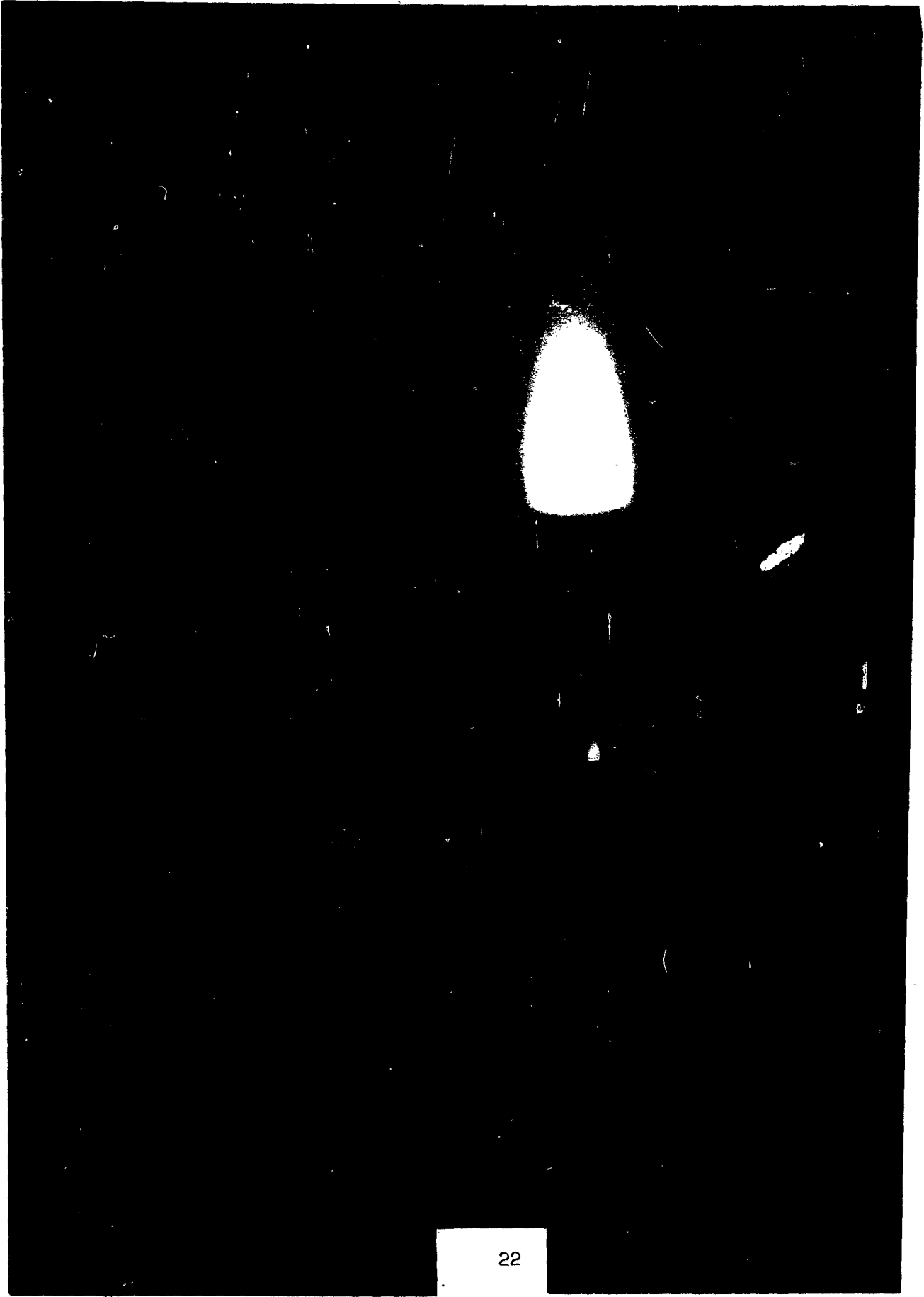
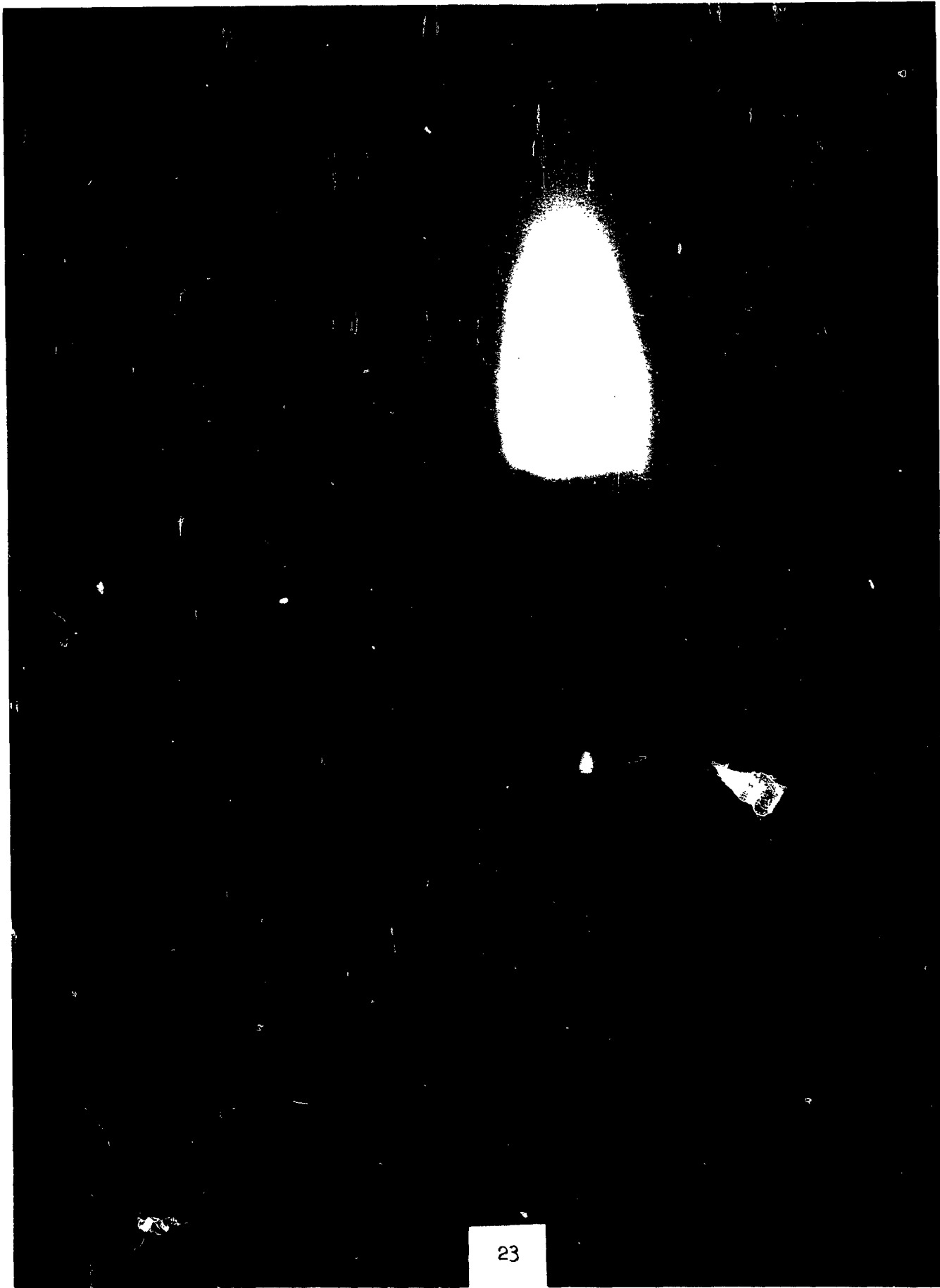


FIGURE 4. Photograph of Flow from a 15° Half-Angle Conical Nozzle  
in a Static Ambient with  $P_e/P_a = 97.0$ .



23

FIGURE 5. Photograph of Flow from a  $15^\circ$  Half-Angle Conical Nozzle  
in a Static Ambient with  $P_e/P_a = 136.5$ .

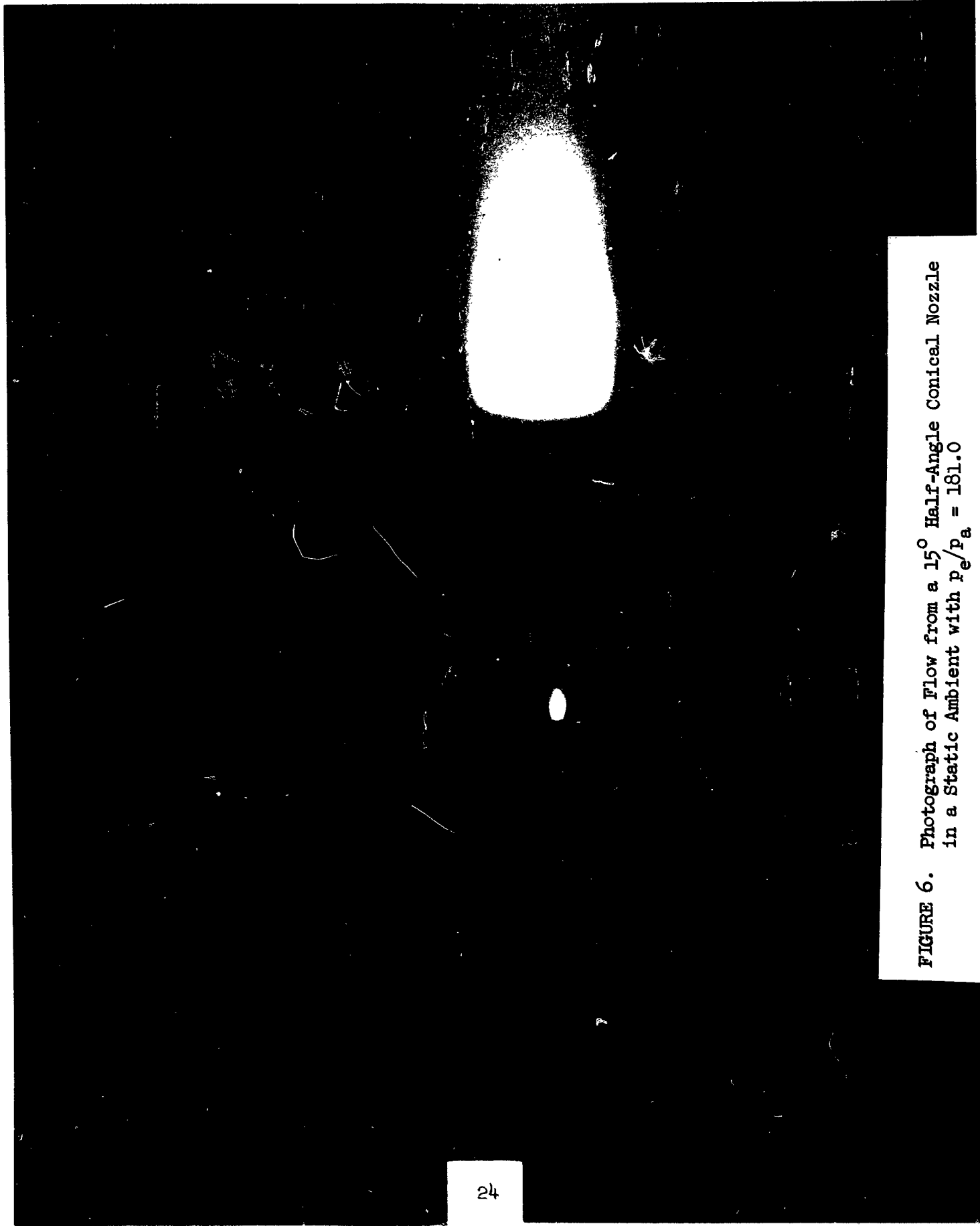


FIGURE 6. Photograph of Flow from a  $15^\circ$  Half-Angle Conical Nozzle  
in a Static Ambient with  $p_e/p_a = 181.0$

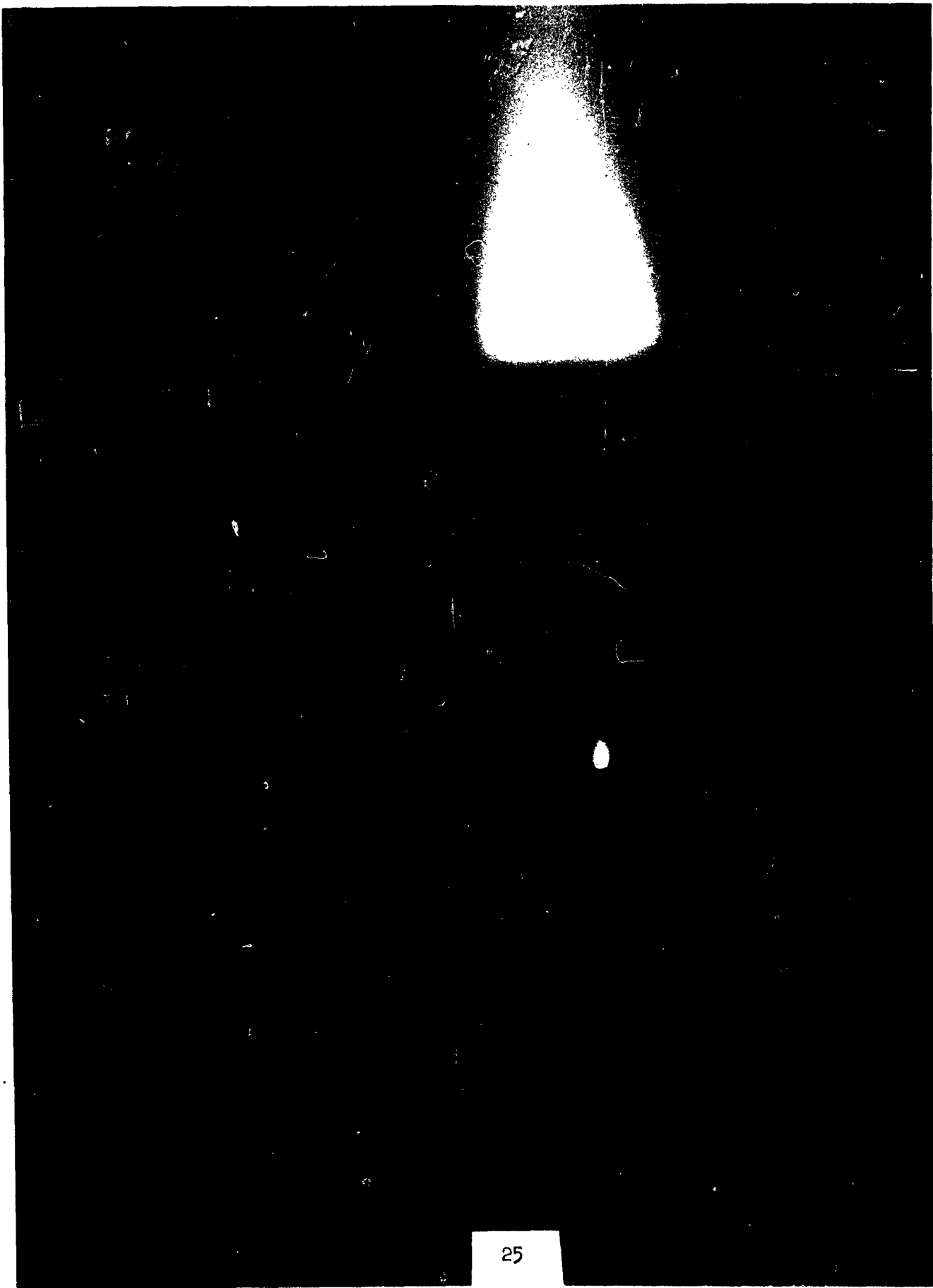


FIGURE 7. Photograph of Flow from a  $15^\circ$  Half-Angle Conical Nozzle  
in a Static Ambient with  $p_e/p_a = 290.0$ .

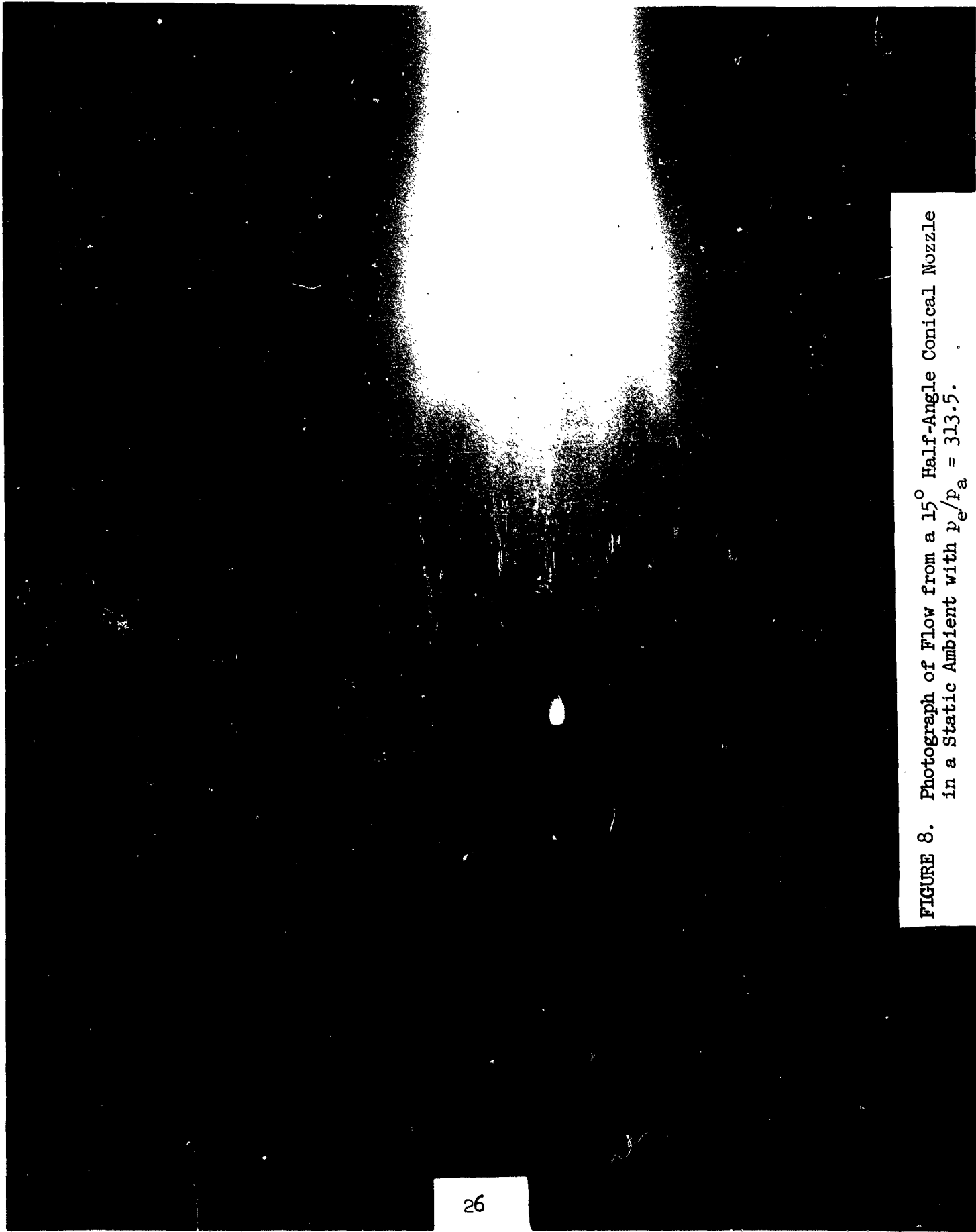


FIGURE 8. Photograph of Flow from a  $15^\circ$  Half-Angle Conical Nozzle  
in a Static Ambient with  $p_e/p_a = 313.5$ .

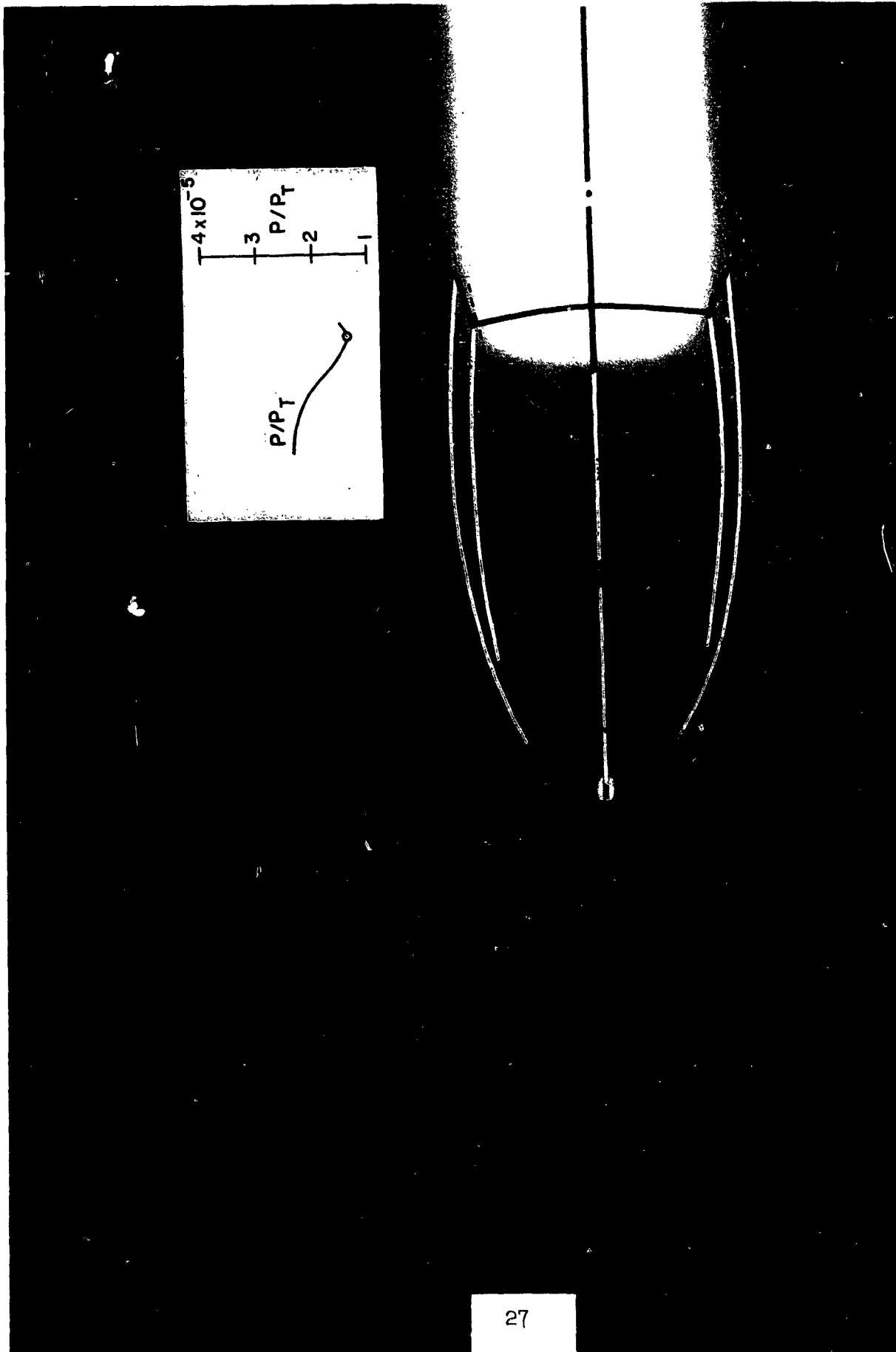


FIGURE 9. Photograph of Flow from a  $15^\circ$  Half-Angle Conical Nozzle in a Static Ambient with  $p_e/p_a = 333.8$ . Superimposed are the jet boundary and incident jet shock (white lines), the Mach disc and reflected shock (solid black lines), and the flow lines (dashed black lines) as calculated by the method of Bowyer, D'Attorre, and Yoshihara. Also shown is the variation of the static pressure behind the incident shock.



FIGURE 10. Photograph of Flow from a  $15^\circ$  Half-Angle Conical Nozzle in a Static Ambient  
with  $p_e/p_a = 506.0$ .

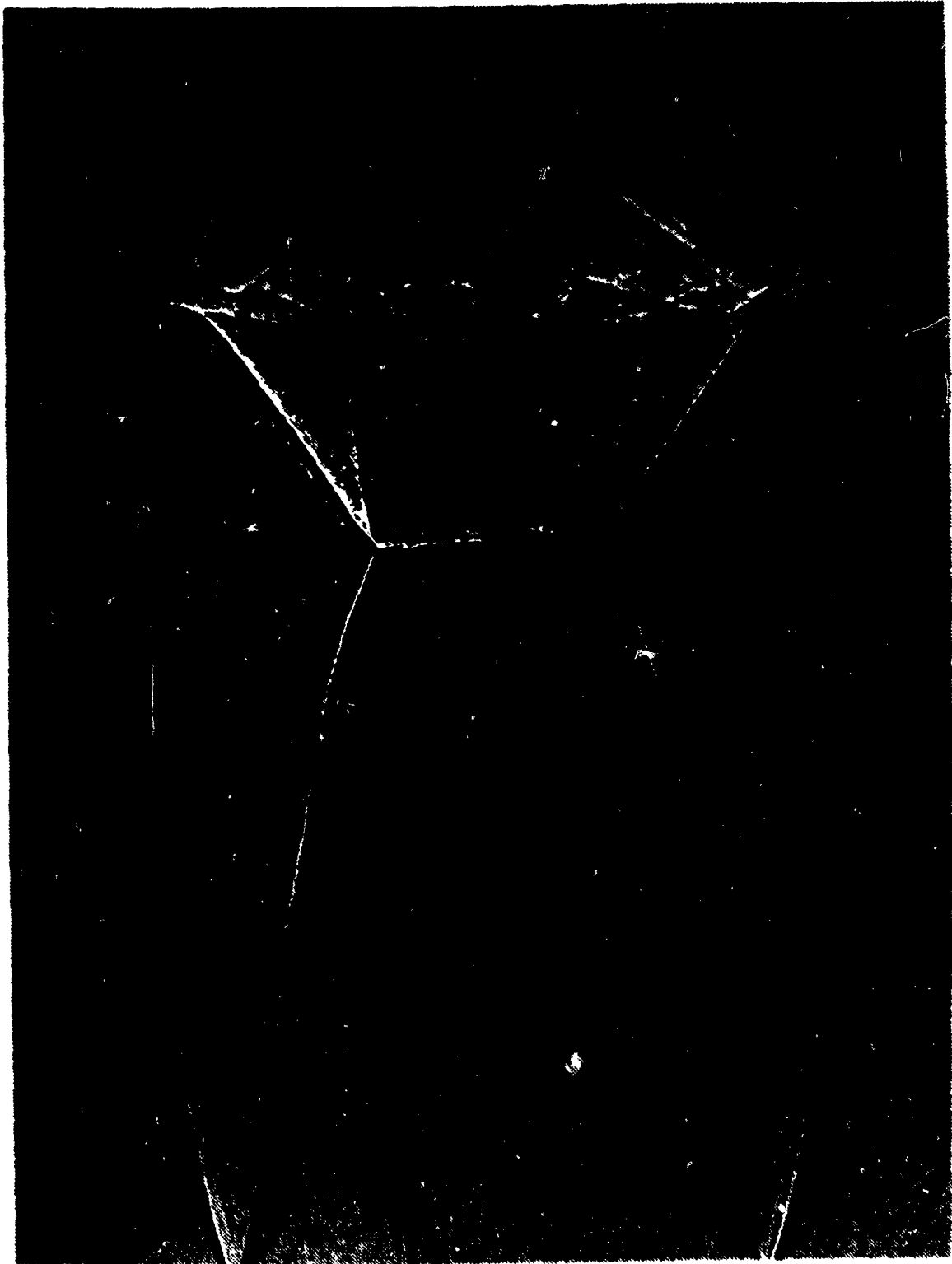


FIGURE 11. Shadowgraph of an Axially Symmetric Air Jet Flowing from a Round Orifice of 10 mm Diameter at a Reservoir Gauge Pressure of 70 lb/in.<sup>2</sup> (reproduced from Reference 9). Superimposed are calculated slopes for the incident shock, reflected shock, Mach disc, and slip line locally at the triple-point (by the technique of Bowyer, D'Attorre, and Yoshihara).



FIGURE 12. A Photograph (Negative) of a Single Engine Missile at a Flight Mach Number of 4.325, at an Exit to Ambient Static Pressure Ratio of 103.5, and at a View Aspect Angle of  $56^{\circ}$ .

AREA RATIO 8:1     $\gamma_e = 1.225$      $\theta_e = 0^\circ$   
 STILL AMBIENT  
 PRESS. RATIO     $P_e/P_0 = 4.68$

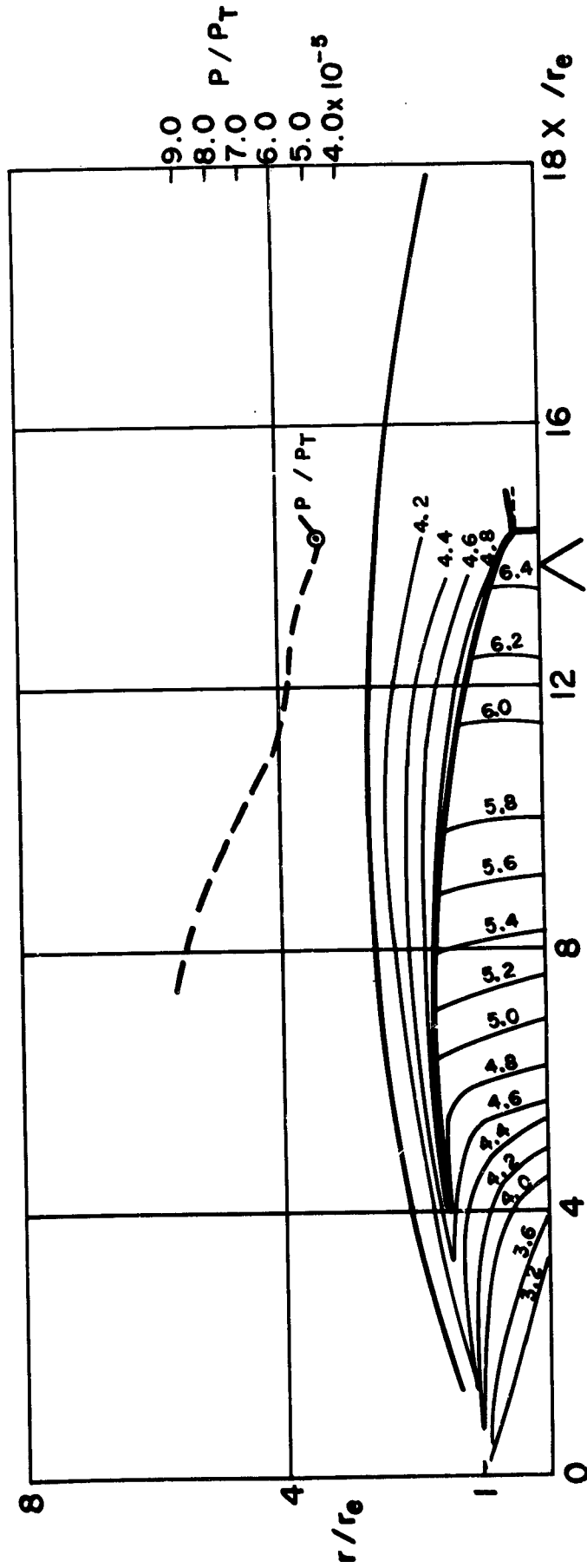


FIGURE 13. Calculated Inviscid Flow Field. Included are the Mach disc, slip line, incident and reflected shock, jet boundary, and lines of constant Mach number as a function of position given by the Bowyer program<sup>11</sup> and the technique of Bowyer, D'Attorre, and Yoshihara. Provided also is the variation of the static pressure behind the incident shock (with the circle denoting the minimum) and the required position of a normal shock to bring the shocked gas up to the ambient pressure (inverted carrot).

AREA RATIO 8:1     $\gamma_e = 1.225$      $\theta_e = 0^\circ$   
 STILL AMBIENT  
 PRESS. RATIO  $P_e/P_0 = 10.3$

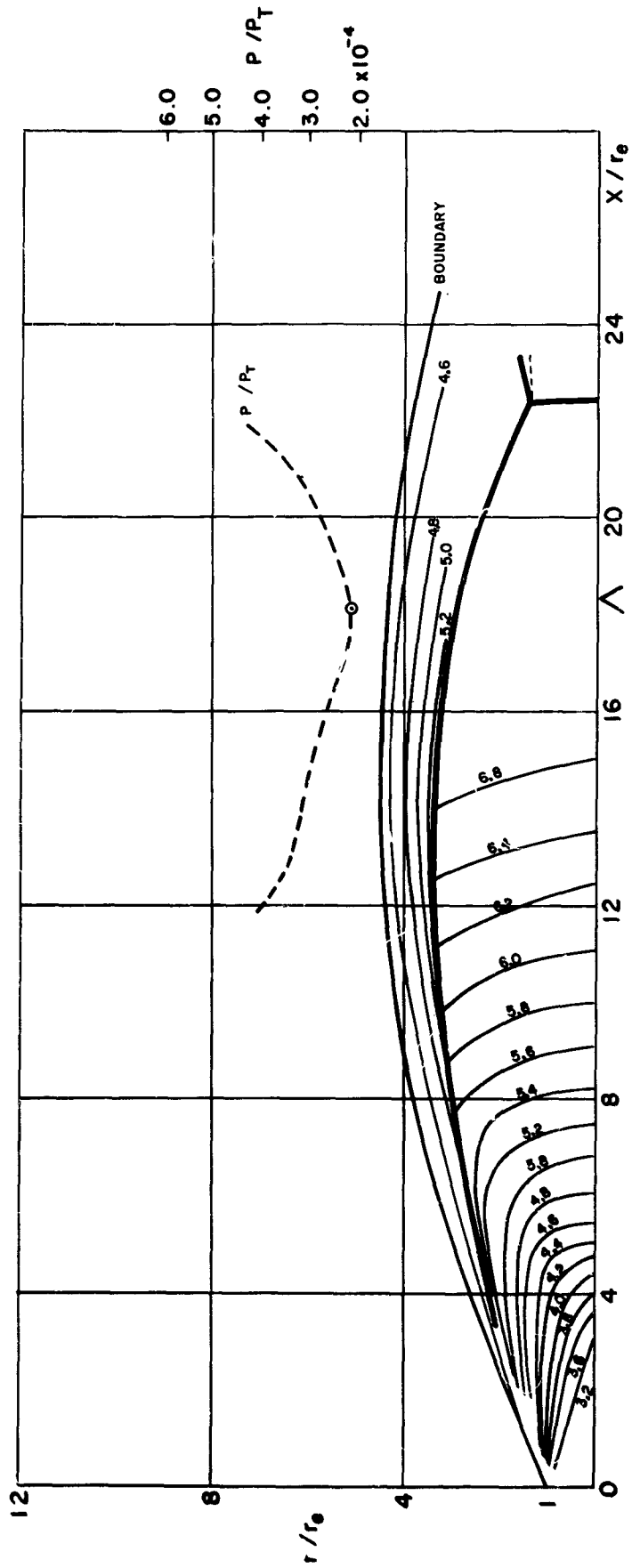


FIGURE 14. Calculated Inviscid Flow Field. Included are the Mach disc, slip line, incident and reflected shock, jet boundary, and lines of constant Mach number as a function of position given by the Bowyer program<sup>11</sup> and the technique of Bowyer, D'Atorre, and Yoshihara. Provided also is the variation of the static pressure behind the incident shock (with the circle denoting the minimum) and the required position of a normal shock to bring the shocked gas up to the ambient pressure (inverted carrot).

AREA RATIO 8:1     $\gamma_e = 1.225$      $\theta_e = 0^\circ$   
 STILL AMBIENT  
 PRESS. RATIO     $P_e / P_0 = 25.4$

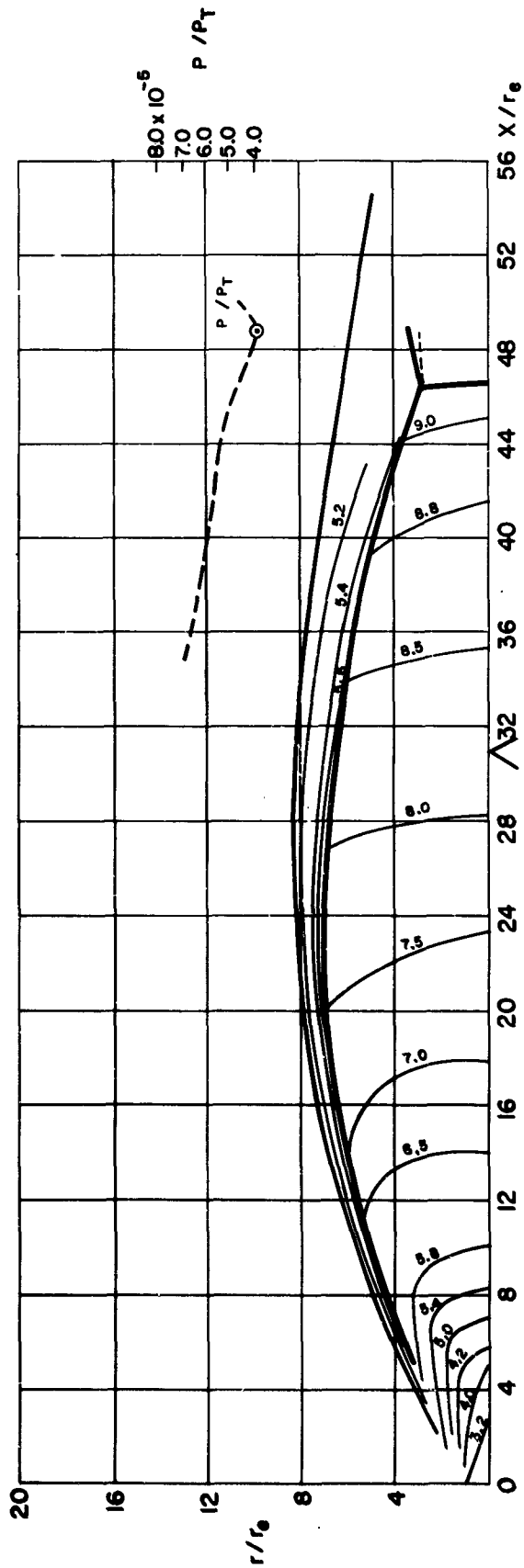


FIGURE 15. Calculated Inviscid Flow Field. Included are the Mach disc, slip line, incident and reflected shock, jet boundary, and lines of constant Mach number as a function of position given by the Bowyer program<sup>11</sup> and the technique of Bowyer, D'Atorre, and Yoshihara. Provided also is the variation of the static pressure behind the incident shock (with the circle denoting the minimum) and the required position of a normal shock to bring the shocked gas up to the ambient pressure (inverted carrot).

AREA RATIO  $\delta:1$   $\gamma_e = 1.225$   $\theta_e = 0^\circ$   
 STILL AMBIENT  
 PRESS. RATIO  $P_0 / P_\infty = 50.1$

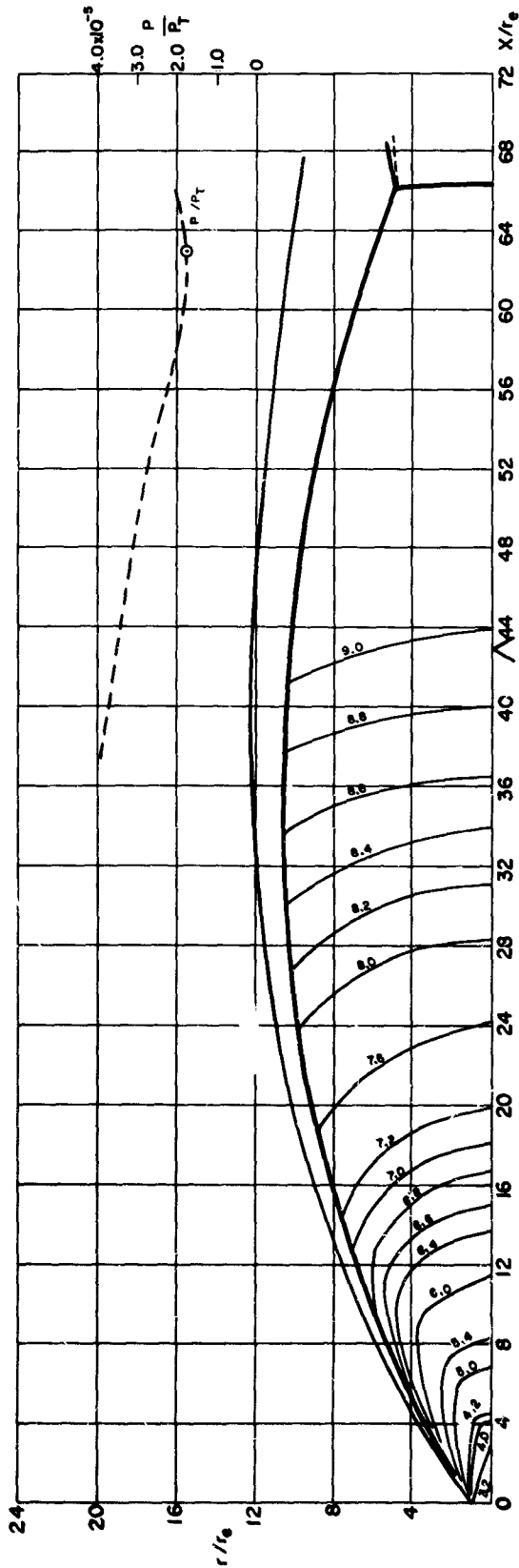


FIGURE 16. Calculated Inviscid Flow Field. Included are the Mach disc, slip line, incident and reflected shock, jet boundary, and lines of constant Mach number as a function of position given by the Bowyer program<sup>11</sup> and the technique of Bowyer, D'Atorre, and Yoshihara. Provided also is the variation of the static pressure behind the incident shock (with the circle denoting the minimum) and the required position of a normal shock to bring the shocked gas up to the ambient pressure (inverted carrot).

AREA RATIO 8 : 1     $\gamma_e = 1.225$      $\theta_e = 0^\circ$   
 STILL AMBIENT  
 PRESS. RATIO  $P_e / P_a = 104.0$

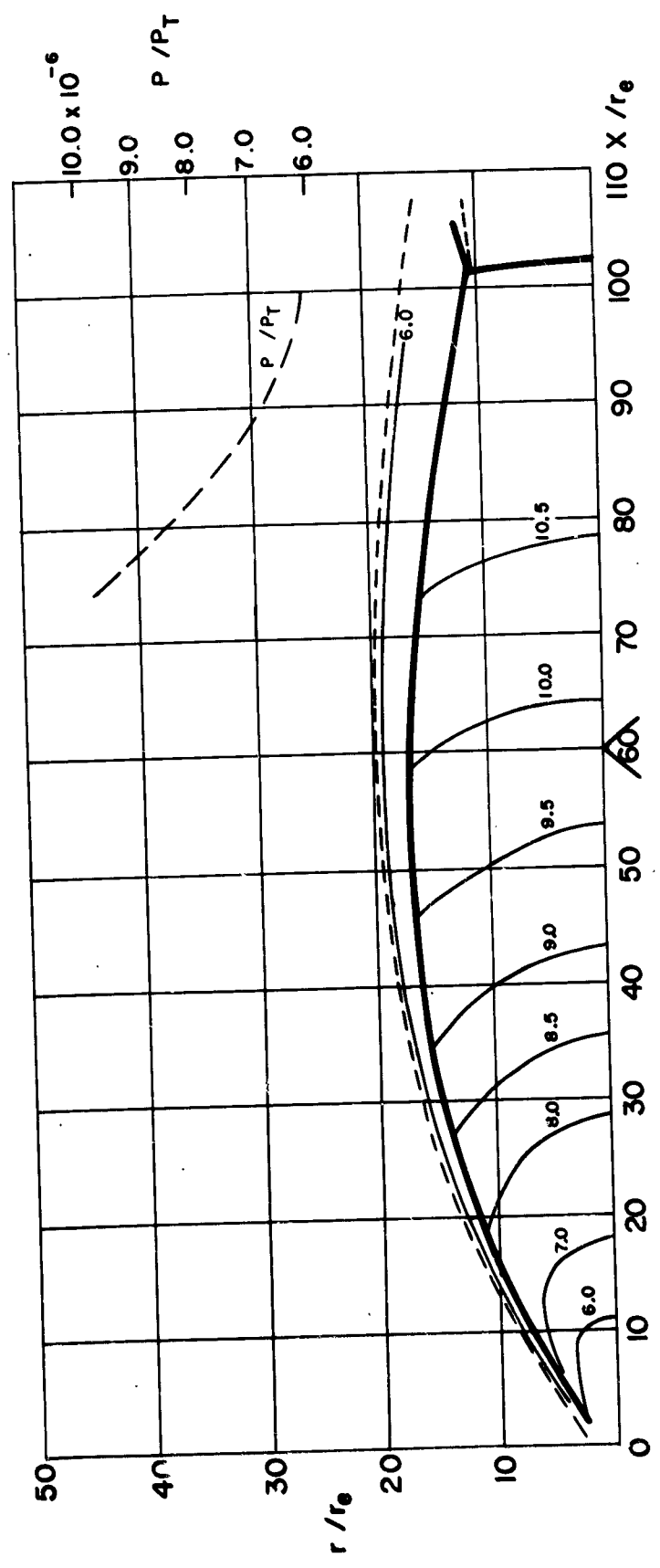


FIGURE 17. Calculated Inviscid Flow Field. Included are the Mach disc, slip line, incident and reflected shock, jet boundary, and lines of constant Mach number as a function of position given by the Bowyer program<sup>11</sup> and the technique of Bowyer, D'Attorre, and Yoshihara. Provided also is the variation of the static pressure behind the incident shock (with the circle denoting the minimum) and the required position of a normal shock to bring the shocked gas up to the ambient pressure (inverted carrot).

AREA RATIO 8:1  $\gamma_e = 1.225$   $\theta_e = 0^\circ$   
 FREE STREAM MACH NUMBER 1.75  
 PRESS. RATIO  $P_e / P_a = 4.68$

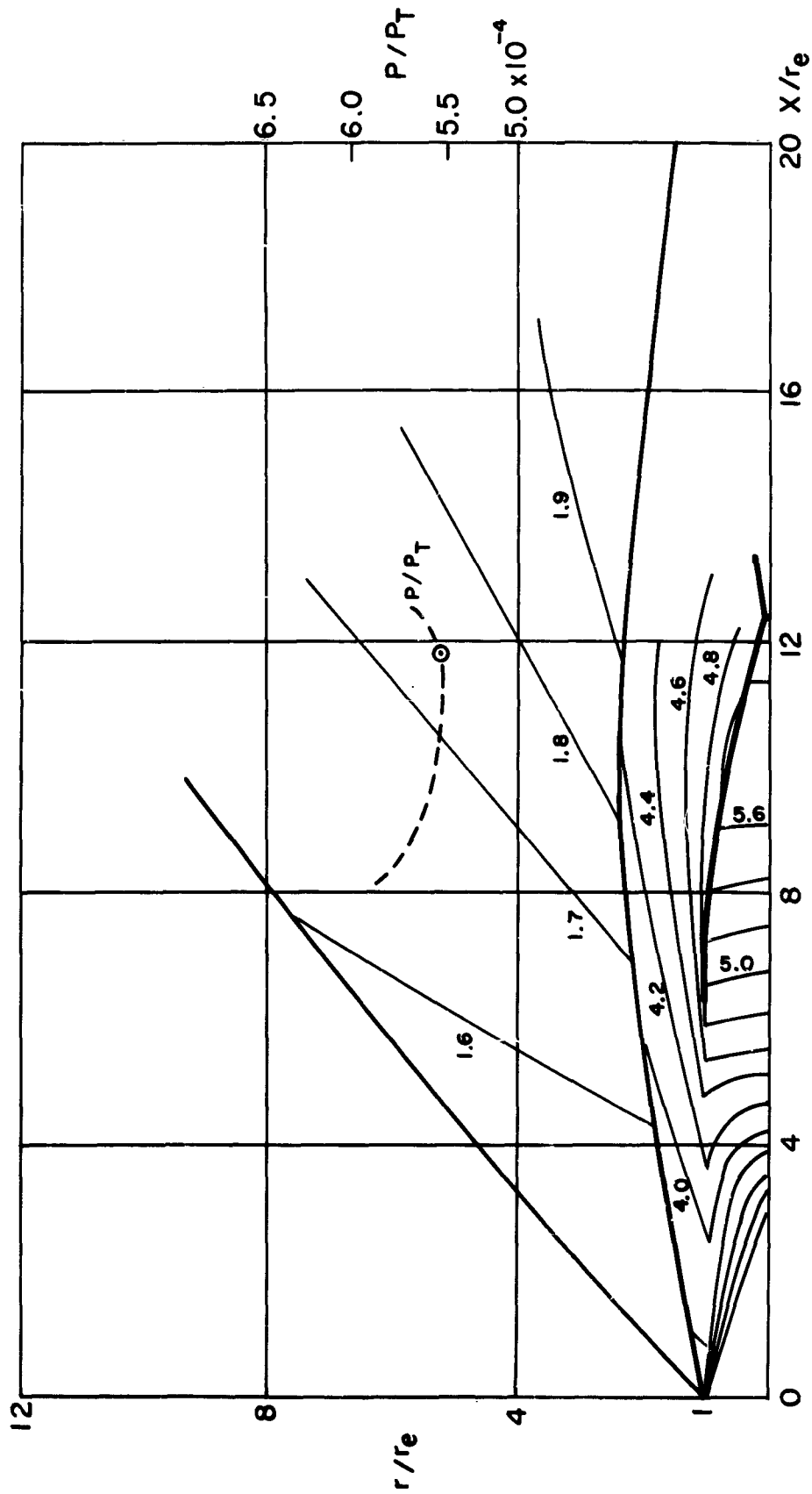


FIGURE 18. Calculated Inviscid Flow Field. Included are the Mach disc, slip line, incident and reflected shock, jet boundary, air shock, and lines of constant Mach number as a function of position given by the Bowyer program<sup>11</sup> and the technique of Bowyer, D'Atorre, and Yoshihara. Provided also is the variation of the static pressure behind the incident shock (with the circle denoting the minimum) and the required position of a normal shock to bring the shocked gas up to the ambient pressure (inserted comment)

AREA RATIO 8:1  $\gamma_e = 1.225$   $\theta_e = 0^\circ$   
 FREE STREAM MACH NUMBER 1.75  
 PRESS. RATIO  $P_e / P_a = 4.68$

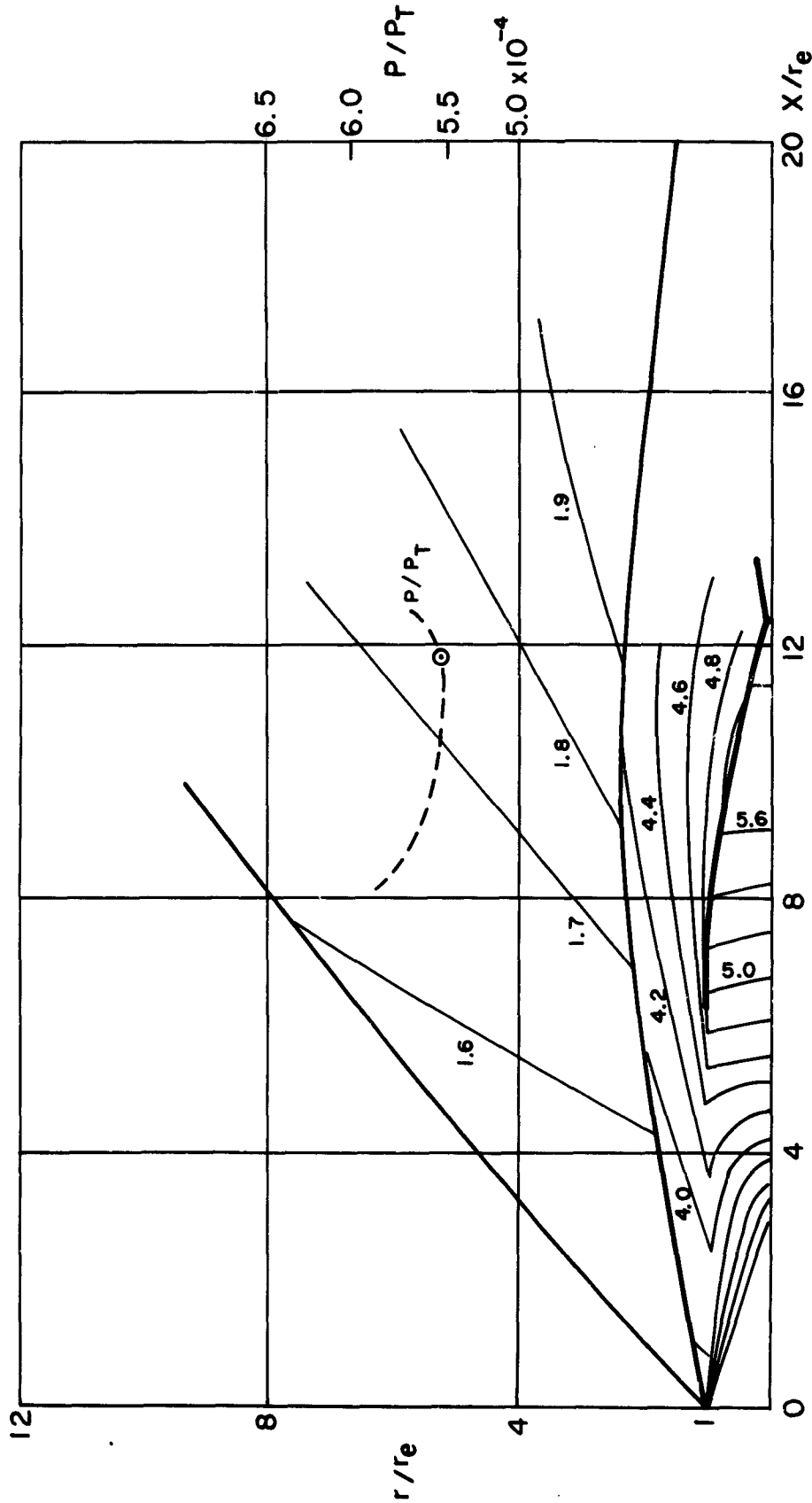


FIGURE 18. Calculated Inviscid Flow Field. Included are the Mach disc, slip line, incident and reflected shock, jet boundary, air shock, and lines of constant Mach number as a function of position given by the Bowyer program<sup>11</sup> and the technique of Bowyer, D'Atorre, and Yoshihara. Provided also is the variation of the static pressure behind the incident shock (with the circle denoting the minimum) and the required position of a normal shock to bring the shocked gas up to the ambient pressure (inverted carrot).

AREA RATIO 8:1  $\gamma_e = 1.225$   $\theta_e = 0^\circ$   
 FREE STREAM MACH NUMBER 2.25  
 PRESS. RATIO  $P_e / P_a = 10.3$

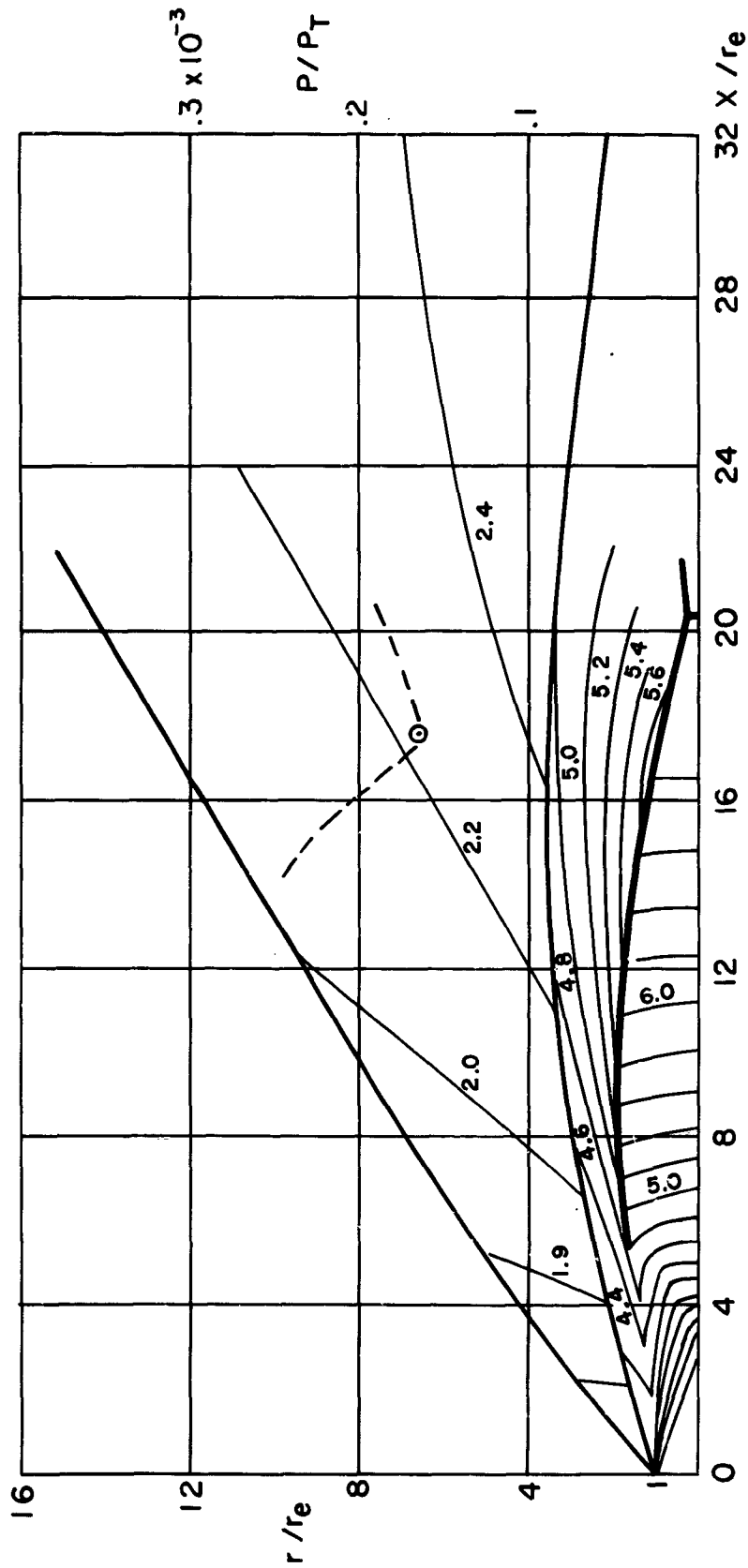


FIGURE 19. Calculated Inviscid Flow Field. Included are the Mach disc, slip line, incident and reflected shock, jet boundary, air shock, and lines of constant Mach number as a function of position given by the Bowyer program<sup>11</sup> and the technique of Bowyer, D'Atorre, and Yoshihara. Provided also is the variation of the static pressure behind the incident shock (with the circle denoting the minimum) and the required position of a normal shock to bring the shocked gas up to the ambient pressure (inverted carrot).

AREA RATIO 8:1  $\gamma_e = 1.225$   $\theta_e = 0^\circ$   
 FREE STREAM MACH NUMBER 3.55  
 PRESS. RATIO  $P_e / P_a = 10.3$

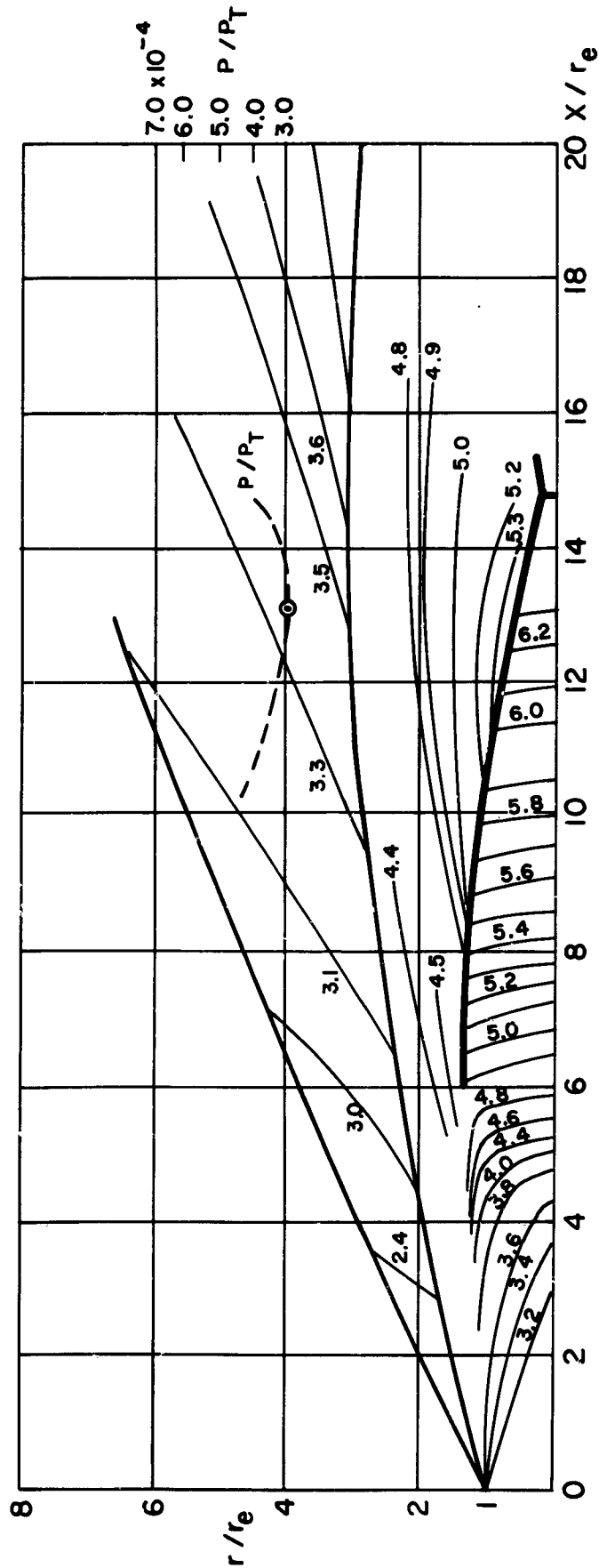


FIGURE 20. Calculated Inviscid Flow Field. Included are the Mach disc, slip line, incident and reflected shock, jet boundary, air shock, and lines of constant Mach number as a function of position given by the Bowyer program<sup>11</sup> and the technique of Bowyer, D'Atorre, and Yoshihara. Provided also is the variation of the static pressure behind the incident shock (with the circle denoting the minimum) and the required position of a normal shock to bring the shocked gas up to the ambient pressure (inverted carrot).

AREA RATIO 8 : 1     $\gamma_e = 1.225$      $\theta_e = 0^\circ$   
 FREE STREAM MACH NUMBER 2.75  
 PRESS. RATIO  $P_e / P_a = 25.4$

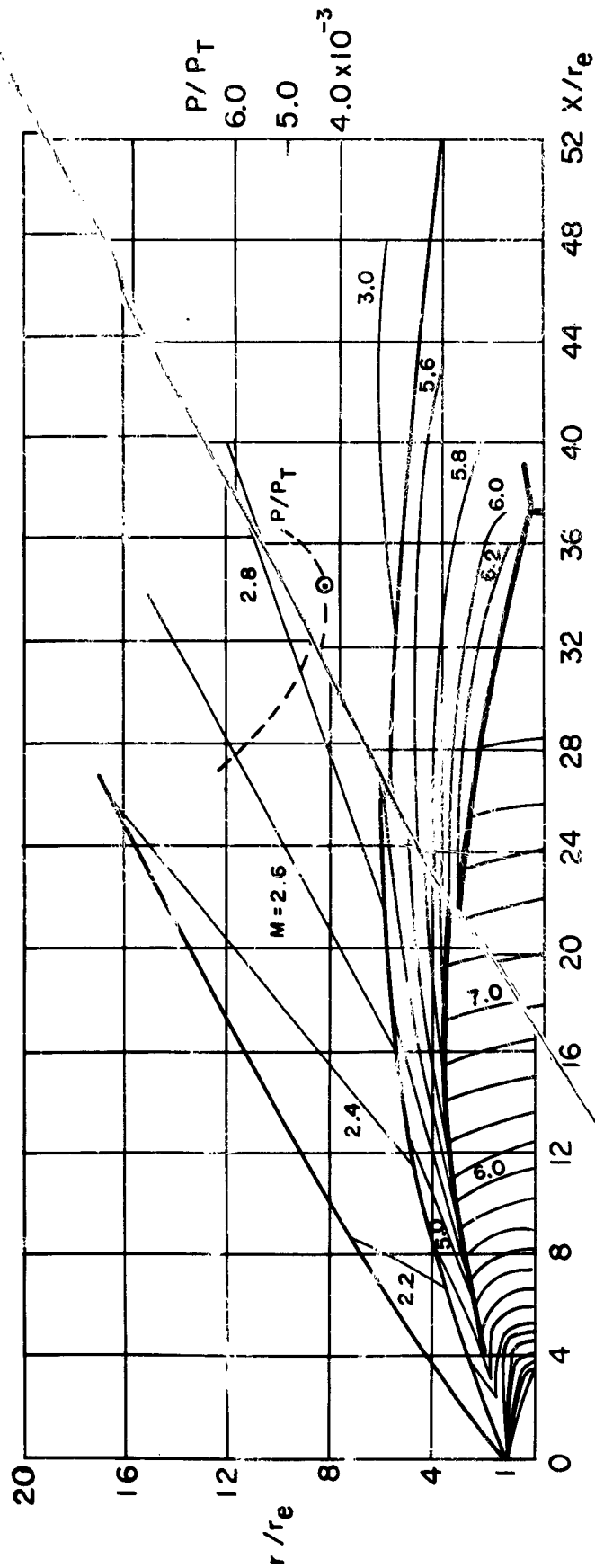


FIGURE 21. Calculated Inviscid Flow Field. Included are the Mach disc, slip lines, incident and reflected shock, jet boundary, air shock, and lines of constant Mach number as a function of position given by the Bowyer program<sup>11</sup> and the technique of Bowyer, D'Astorre, and Yoshihara. Provided also is the variation of the static pressure behind the incident shock (with the circle denoting the minimum) and the required position of a normal shock to bring the shocked gas up to the ambient pressure (inverted carrot).

AREA RATIO 8 : 1     $\gamma_e = 1.225$      $\theta_e = 0^\circ$   
 FREE STREAM MACH NUMBER 3.25  
 PRESS. RATIO  $P_e / P_a = 50.1$

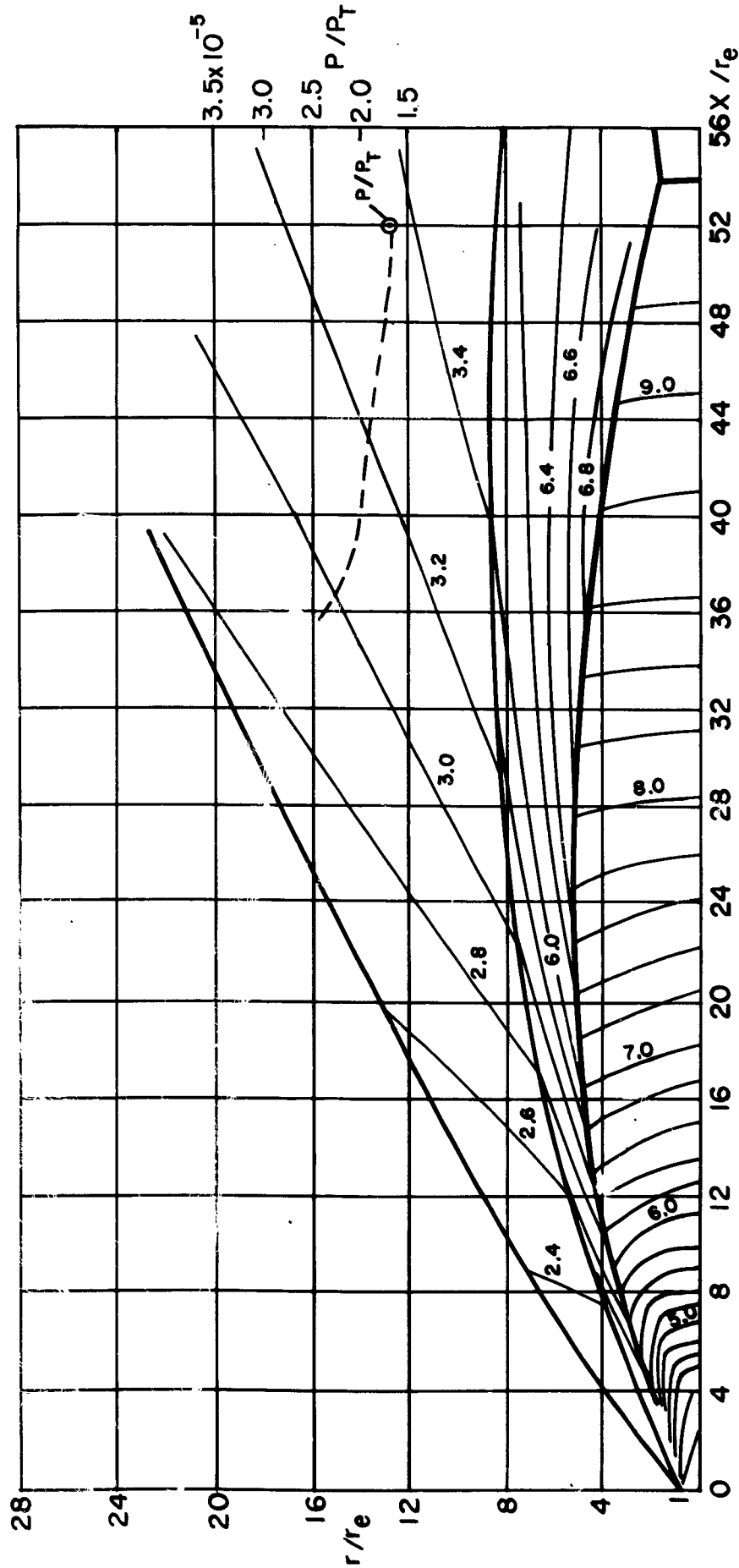


FIGURE 22. Calculated Inviscid Flow Field. Included are the Mach disc, slip line, incident and reflected shock, jet boundary, air shock, and lines of constant Mach number as a function of position given by the Bowyer program and the technique of Bowyer, D'Atorre, and Yoshihara. Provided also is the variation of the static pressure behind the incident shock (with the circle denoting the minimum) and the required position of a normal shock to bring the shocked gas up to the ambient pressure (inverted carrot).

AREA RATIO 8 : 1     $\gamma_e = 1.225$      $\theta_e = 0^\circ$   
 FREE STREAM MACH NUMBER 4.33  
 PRESS. RATIO  $P_e / P_a = 104.0$

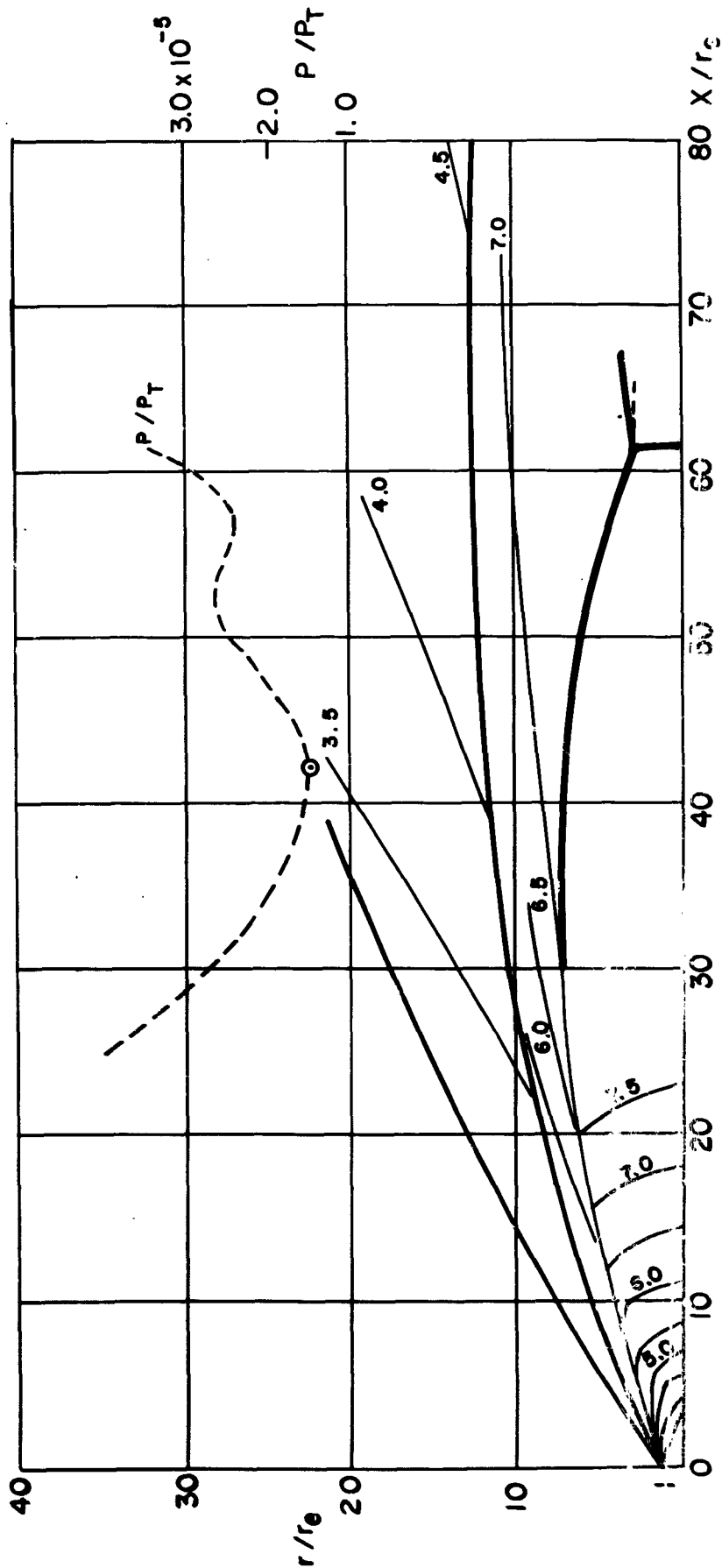


FIGURE 23. Calculated Inviscid Flow Field. Included are the Mach disc, slip line, incident and reflected shock, jet boundary, air shock, and lines of constant Mach number as a function of position given by the Bowyer program<sup>11</sup> and the technique of Bowyer, D'Attorre, and Yoshihara. Provided also is the variation of the static pressure behind the incident shock (with the circle denoting the minimum) and the required position of a normal shock to bring the shocked gas up to the ambient pressure (inverted carrot).